



NOAA Technical Memorandum NMFS F/NWC-168

Tuning of the OSCURS Numerical Model to Ocean Surface Current Measurements in the Gulf of Alaska

by
W. James Ingraham, Jr.
and
Robert K. Miyahara

August 1989

U.S. DEPARTMENT OF COMMERCE
National Oceanic and Atmospheric Administration
National Marine Fisheries Service

This TM series is used for documentation and timely communication of preliminary results, interim reports, or special purpose information, and has not received complete formal review, editorial control, or detailed editing.

TUNING OF THE OSCURS NUMERICAL MODEL TO OCEAN
SURFACE CURRENT MEASUREMENTS IN THE GULF OF ALASKA

by

W. James Ingraham, Jr.

and

Robert K. Miyahara

Resource Ecology and Fisheries Management Division
Alaska Fisheries Science Center
National Marine Fisheries Service
National Oceanic and Atmospheric Administration
7600 Sand Point Way N.E.
Seattle, WA 98115

August 1989

i.a

THIS PAGE INTENTIONALLY LEFT BLANK

ABSTRACT

We reassessed an empirical model for numerical-ocean surface current simulations (OSCURS) that was developed in 1988 to analyze variability in Lagrangian drift in the North Pacific Ocean and Bering Sea (north of lat. 35°N). The model, which computes currents from the vector sum of geostrophic current plus wind drift was tuned with data from the Gulf of Alaska, collected in 1978 with satellite tracked drifters drogued at 20 m. By applying incremented linear tuning coefficients to find the best fit, we evaluate its sensitivity to several functions for computing drift speed and angle of deflection of the current to the right of the wind. The best agreement was obtained using 1.2 times Witting's formula $(4.8\sqrt{W})$ for drift speed and either a constant 25 degrees or Weber's function for the angle of deflection to the right of the wind. Despite limitations due to the computation of winds from Fleet Numerical Oceanography Center gridded sea level pressure data, the 90 km grid size, and the once daily time step, we obtained remarkably good visual agreement between the model's progressive vector tracks and two out of the three drifters available. Although we have not tuned OSCURS to data from the Bering Sea or other parts of the North Pacific Ocean, we are confident that this model can accurately simulate ocean currents in the mixed layers of areas other than the Gulf of Alaska.

THIS PAGE INTENTIONALLY LEFT BLANK

CONTENTS

	Page
INTRODUCTION.....	1
THE INITIAL UNTUNED OSCURS MODEL	2
Daily Surface Current Fields	4
Geostrophic Currents	4
Ocean Currents Due to Computed Wind	7
Total Ocean Currents	12
Progressive Displacement Vectors.....	15
Geostrophic Currents.....	16
Wind Drift	19
Total Drift Versus Drifter Data	21
REASSESSMENT OF DRIFT CALCULATIONS.....	29
Speed of Drift Driven by Wind Speed	29
Clockwise Angle of Deflection	38
Final Tuning Factors	46
REFERENCES	65

INTRODUCTION

The OSCURS (Ocean Surface Current Simulations) numerical model was formulated by Ingraham and Miyahara (1988) as a tool in developing an empirical index of ocean variability for use in fisheries management and ecosystem modeling research in the North Pacific Ocean and Bering Sea. Since the initial document was completed, we have improved the model by testing other empirical formulae for estimating surface drift in the mixed layer and tuning of the model output to available ocean current measurements (satellite tracked drifters).

We report here the results of new functions for angle of deflection to the right of the wind and linear tuning factors for speed and update the model with the best-fit coefficients. Although the complete model extends ocean-wide from Seattle to Tokyo, we focus this first attempt to tune the model in the Gulf of Alaska, where the first set of satellite tracked drifter measurements was made in July 1978 (Reed 1980). We will examine the portion of the model in the Bering Sea and the central and western North Pacific Ocean in subsequent publications as calibration data become available. The results presented here have increased our confidence that these model simulations of ocean surface currents reflect ocean conditions well enough to be useful, especially for variability studies.

THE INITIAL UNTUNED OSCURS MODEL

The basic function of the OSCURS Model is to compute surface currents by vector addition of geostrophic flow and wind drift on a spatial resolution of about 85 km and to compute using a daily time step. Although a- somewhat smaller spatial resolution would have resolved some small-scale oceanographic features, our broad-based fisheries interests required oceanwide coverage to encompass the migrations of wide-ranging stocks. In order to optimize computer storage and computational time, we used an orthogonal grid (40X104) of about 85 km (Fig. 1). To minimize the effects of the long grid length, we used a two-dimensional, four-point Bessel function to interpolate between grid points and amplified geostrophic currents in areas of narrow (subgrid size) coastal boundary currents, particularly in the Alaskan Stream south of the Alaskan Peninsula and the Aleutian Islands. We hoped that the small, daily time step would allow us to detect significant details about flow features probably masked by the longer time averages of previous studies which used seasonal means (Emery and Hamilton 1985) or monthly means (Emery et al. 1985) of sea level pressure in their discussion of variability.

Although the bulk of the computations is devoted to obtaining the total velocity field for any selected day in our historical sea level pressure file between 1946 and 1987, the highlight of this model's results has been its ability to go to any location in the field (including between grid points) for the given day and compute a representative displacement vector--the

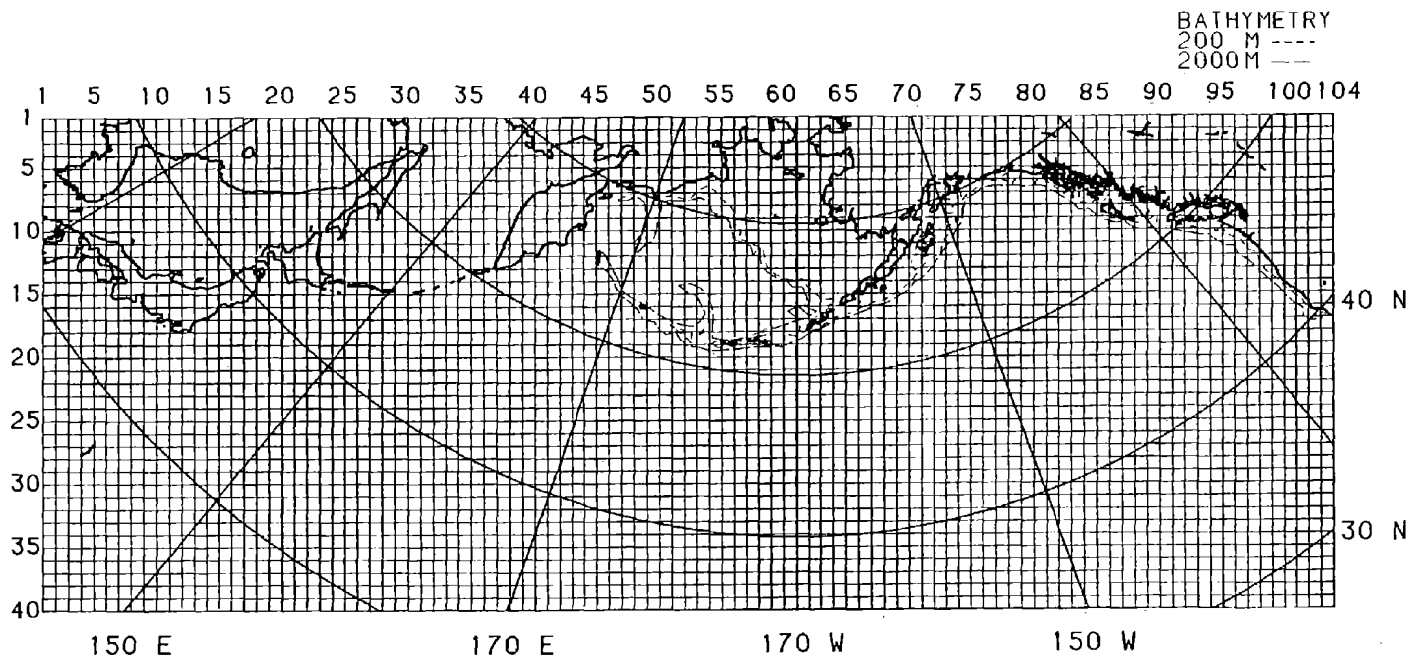


Figure 1.--Grid (83-95 km) of the OSCURS numerical model (40X104).

distance and direction a parcel of water in the mixed layer would move in 24 hours. We produced daily Lagrangian progressive vector trajectories (simulated drifter tracks) in a computational loop of six steps: 1) read in sea level pressure for the selected day, 2) compute wind, 3) compute wind drift current, 4) tune and sum velocity components, 5) add boundary effects, and 6) compute the surface transport vectors. (distance traveled per day) at each of the chosen starting points (the end points of these computed vectors become the starting points for the following day's vectors). We were able to select several tracks with different starting points for each run. The following sections present the essential elements of the initial untuned model.

Daily Surface Current Fields

The daily total current field is the basic unit of OSCURS. Each field is composed from three parts: 1) geostrophic currents, (2) wind drift, and (3) total currents.

Geostrophic Currents

We describe here the derivation and amplification of the geostrophic current field because a portion of the field is used with the wind-induced velocity field to compose the total surface current vector field for the selected year, month, and day.

The first component of velocity comes from a standard calculation (LaFond 1951) of the permanent (long-term mean) geostrophic current (0/3,000 decibar (db)). We obtained long-term mean temperature and salinity values at standard depths

used in the vertical integration of density from 0 to 3,000 m from a 1X1 degree numerical atlas (Bauer and Robinson 1985). Anomalies of dynamic height were horizontally interpolated to obtain values at model grid points. We performed near-shore extrapolations by adjusting stations shallower than the reference level of 3,000 m with the deeper water properties of the nearest offshore station.

The major features of this long-term mean flow (Fig. 2) were consistent with descriptions in other studies (Favorite et al. 1976; Reed and Schumacher 1987). Some highlights included a large area of uneventful or relatively unperturbed easterly drift with speeds of less than 5 cm/sec between 40 N and 50 N from 170 W to about 140 W, and a rather complex divergence in this onshore flow toward the north and south (the Great Divergence). Higher speeds of about 5 cm/sec appear locally in the southerly flow off the California coast and in the northward flow into the Gulf of Alaska on the eastern portion of the Gulf of Alaska Gyre. Maximum speeds of up to 10 cm/sec are found in the Alaskan Stream, which flows southwestward along the continental slope of the Alaskan Peninsula. These speeds appear artificially low due to the relatively large distance (about 85 km) between grid computation points, because speeds of up to at least 60 cm/sec were calculated by Ingraham and Favorite (1968) from very closely spaced (5-10 km) stations taken across the axis of maximum flow in the vicinity of the 2,000 m isobath. We compensated for the grid size limitation of the model by multiplying the geostrophic velocity at specified grid points by constants (Table 1) which

SURFACE OCEAN CURRENTS
GEOSTROPHIC COMPONENT (0/3000 DB)
10_CM/SEC

BATHYMETRY
200 M - - - -
2000M - - - -

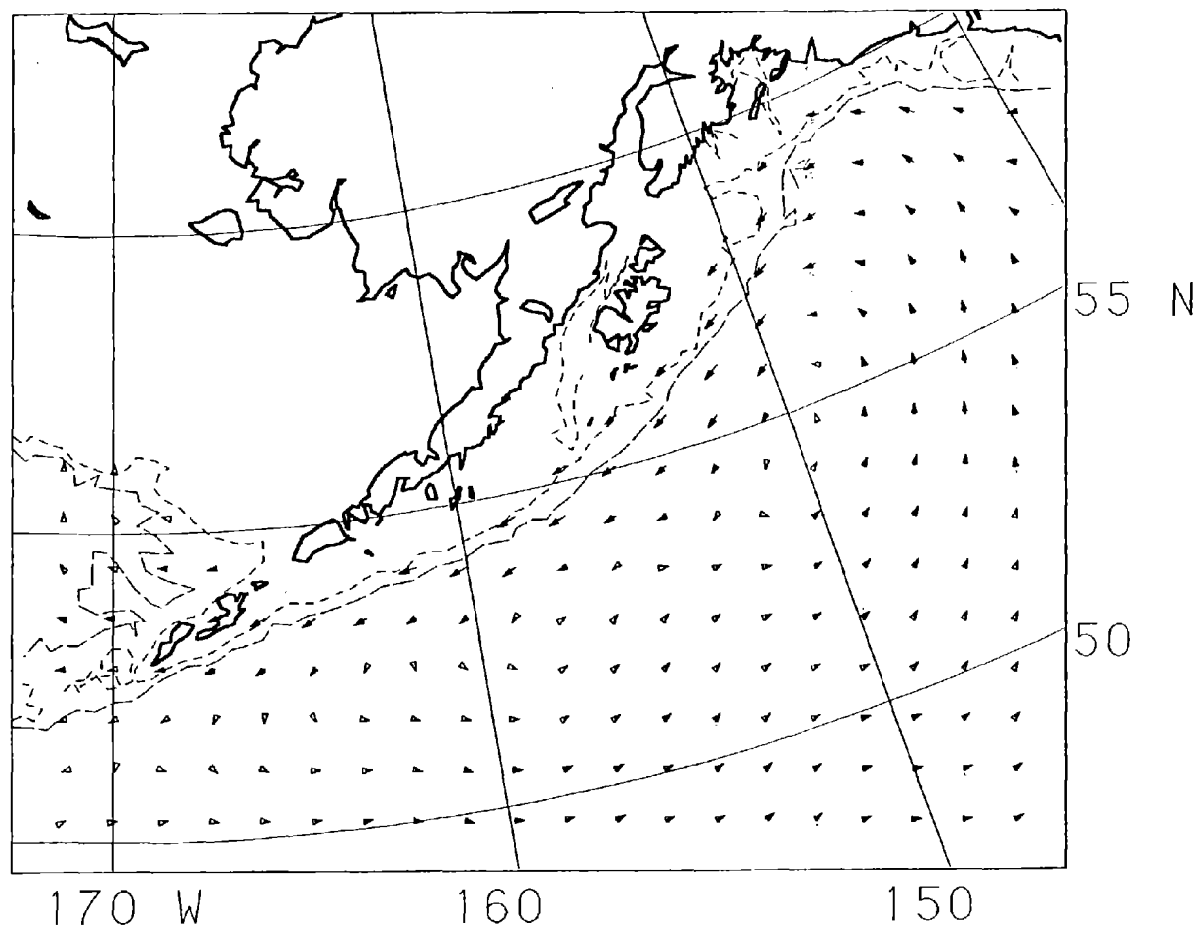


Figure 2.--Geostrophic current vector field calculated from long-term mean anomaly of dynamic height data (0/3,000 db) (cm/sec).

Table 1.--Geostrophic current multipliers at selected I, J grid points (I = 1, 40; J = 1, 104) in the Alaskan Stream.

I	J	Geostrophic current multiplier
9	75	2.00
10	74	6.00
11	74	1.40
11	73	6.00
12	73	2.00
13	72	7.00
14	71	7.00
15	70	4.00
15	69	3.00
16	68	4.00
16	67	4.00
17	66	1.40
17	65	6.00
17	64	2.00
18	63	6.00
18	62	4.00
19	61	5.00
19	60	7.00
19	59	7.00
19	58	6.00
19	57	5.00
19	56	5.00
19	55	5.00
19	54	4.00
19	53	4.00
19	52	3.00

ranged from a maximum of 7.0 at the 2,000 m isobath and decreased to 1.0 (no change) with distance from the 2,000 m isobath. The dominance of the Alaskan Stream as the major current in the velocity field after these coefficients were applied is illustrated in Figure 3. By enhancing only certain grid points near the 2,000 m isobath, we achieved the desired effect of continuous, high-speed flow between the grid points all along the Alaska Peninsula.

Ocean Currents Due to Computed Wind

The second and generally the largest component of velocity is the wind-induced surface drift. We computed this drift in three steps: 1) reading the sea level pressure field for the chosen date, 2) calculating a wind field from the sea level pressure gradient, and 3) calculating a surface current field from an empirical function of the wind speed and direction. Examples of each step for one selected day (17 July 1978) will illustrate the computational methods; for additional details or computer handling procedures, see Ingraham and Miyahara (1988).

We obtained daily (time = 00002) sea level pressure data from the U.S. Navy Fleet Numerical Oceanography Center (FNOC) on their standard 380 km Northern Hemisphere (63X63) grid. The methods used in creating a new time-sequential file (1946 to 1987) of interpolated values at model (40X104) grid points for the model to read is discussed in Ingraham et al. (1983). Wind data were computed after the methods of Larson (1975) using a two-dimensional, numerical, five-point central difference formula

SURFACE OCEAN CURRENTS
GEOSTROPHIC COMPONENT (0/3000 DB)
10 CM/SEC
→

BATHYMETRY
200 M ----
2000 M - - - -

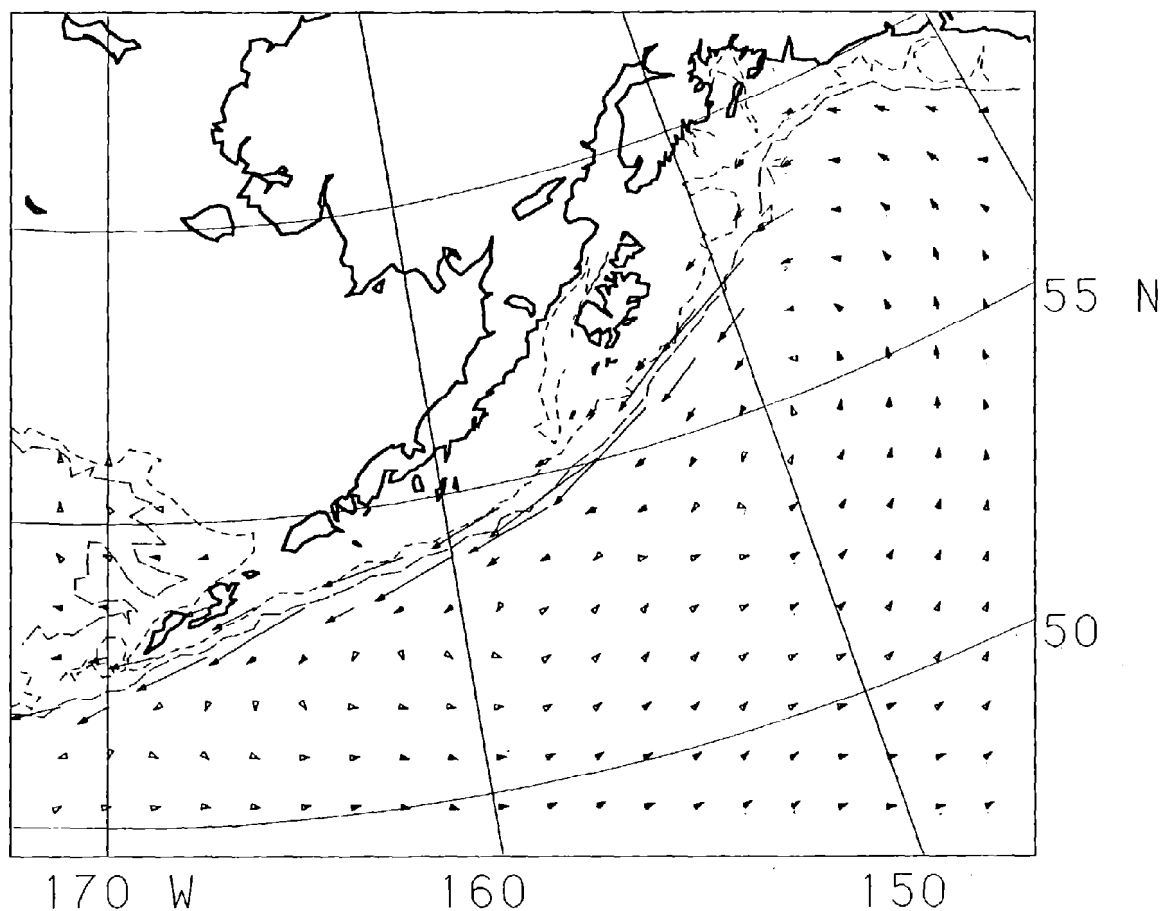


Figure 3. --Geostrophic current vector field (0/3,000 db) (cm/sec).
Amplification factors applied to grid points near the 2,000 m
isobath, the axis of maximum speed in the Alaskan Stream.

to compute the geostrophic wind from the sea level pressure gradient. Dual frictional effects included a deflection angle and speed reduction. The angle of deflection of the wind to the left of the pure geostrophic wind increased toward the south over the grid from about 17 to 23 degrees at low wind speeds, and to about 14 to 17 degrees at higher wind speeds of 20 m/sec. The reduction factor increased toward the north from 15 to 20%. Cross-isobar winds were a dominant feature flowing into the center of low pressure at lat. 50°N, long. 165°W as well as out of the high pressure center at lat. 40°N, long. 142°W (Fig. 4). Although curvature of the isobars changed greatly and the angle of leftward deflection decreased in areas of high wind speeds, a consistent cross-isobar wind remained. At this point, we calculated an ocean current as a direct function of the computed wind.

Although we will treat wind drift computations more extensively in the section on model tuning, we will summarize here the functions used in the original model. Ocean current speed, which has a typical value of about 1 to 3% of the wind speed, was computed by the formula of Witting (1909),

$$C = k\sqrt{W}$$

where C is the speed in centimeters per second due to the wind speed, W, in meters per second and the proportionality constant k is equal to 4.8 for speeds averaged over the mixed layer including wave transport (Hubert and Laevastu 1965). For the angle of deflection to the right of the wind, D, we modified

SURFACE WIND VECTORS
10 M/SEC 7/17/78

BATHYMETRY
200 M - - - -
2000M - - - -

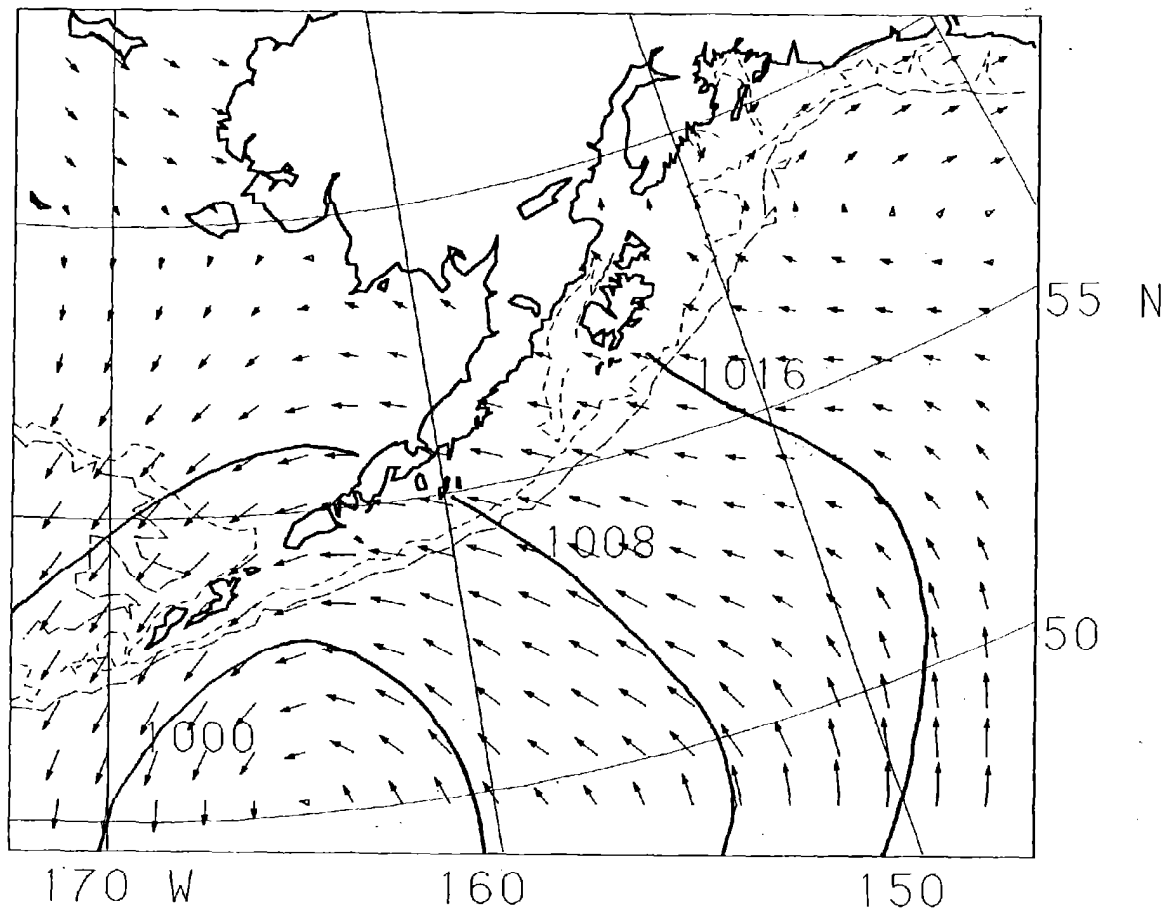


Figure 4.--Wind vector field (m/sec) computed in OSCURS model from arbitrarily selected Fleet Numerical Oceanography Center sea level pressure field for 17 July 1978. Note cross-isobar flow toward lower pressure.

Witting's formula,

$$D=34.0 - 7.5\sqrt{W}$$

to decrease with latitude such that the range of deflection was 22-15 degrees at 5 m/sec, 17-11 degrees at 10 m/sec, 4-3 degrees at 15 m/sec, and zero at winds of 20 m/sec or greater. The deflection of ocean currents to the right of the wind nearly counteracts the deflection of the wind to the left of the geostrophic wind. Ocean currents, therefore, generally appear to be nearly parallel to the sea level pressure isobars (Fig. 5). Notable exceptions are in the areas of highest wind speed (>15-20 m/sec) near lat. 47°N, long. 153°W where the computed deflection angle approaches zero.

Total Ocean Currents

A simple summation of the geostrophic and wind drift components produces the total current vector field for the day. To avoid overshooting of vectors onto land, we applied a logarithmic decrease in speed to zero at the coast and a bending of vectors in the direction of their incidence upon the coast within one grid point distance along the entire coastline. In our tuning exercises, we may apply a multiplicative factor before the summation so that different weights may be applied to each component as desired. This was particularly useful for eliminating one component in order to examine wind or geostrophic effects separately. The wind field dominates the magnitude of the final vectors (Fig. 6), except in the Alaskan Stream, where geostrophic speeds reach 60 cm/sec. Most of the speeds over the

SURFACE OCEAN CURRENTS
(WIND COMPONENT) 7/17/78
10 CM/SEC

BATHYMETRY
200 M - - - -
2000M - - - -

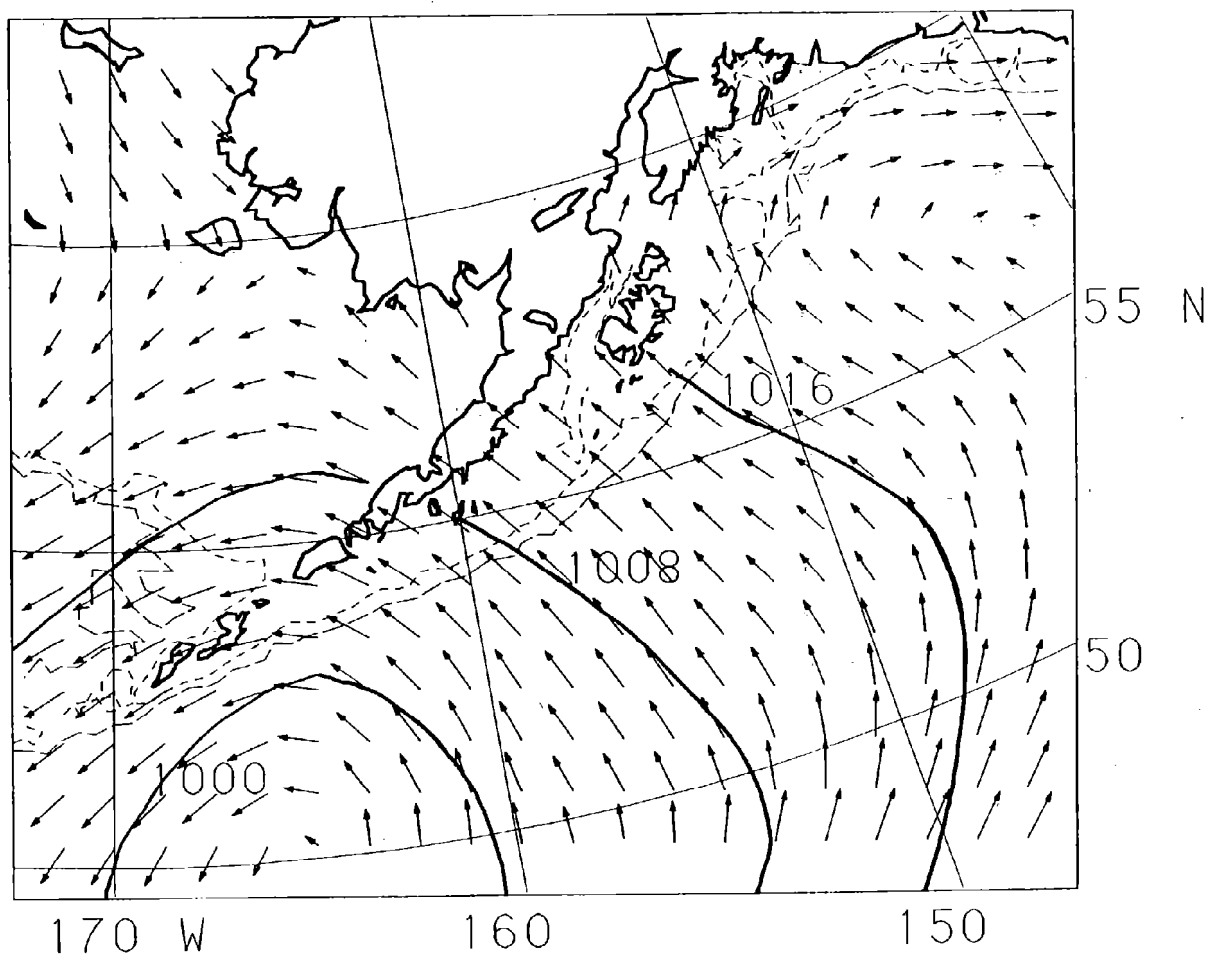


Figure 5.--Surface ocean current vector field (cm/sec) calculated from wind vector field of Figure 4. Note the deflection of the currents to the right of the wind vectors, bringing them closely in line with isobars of sea level pressure.

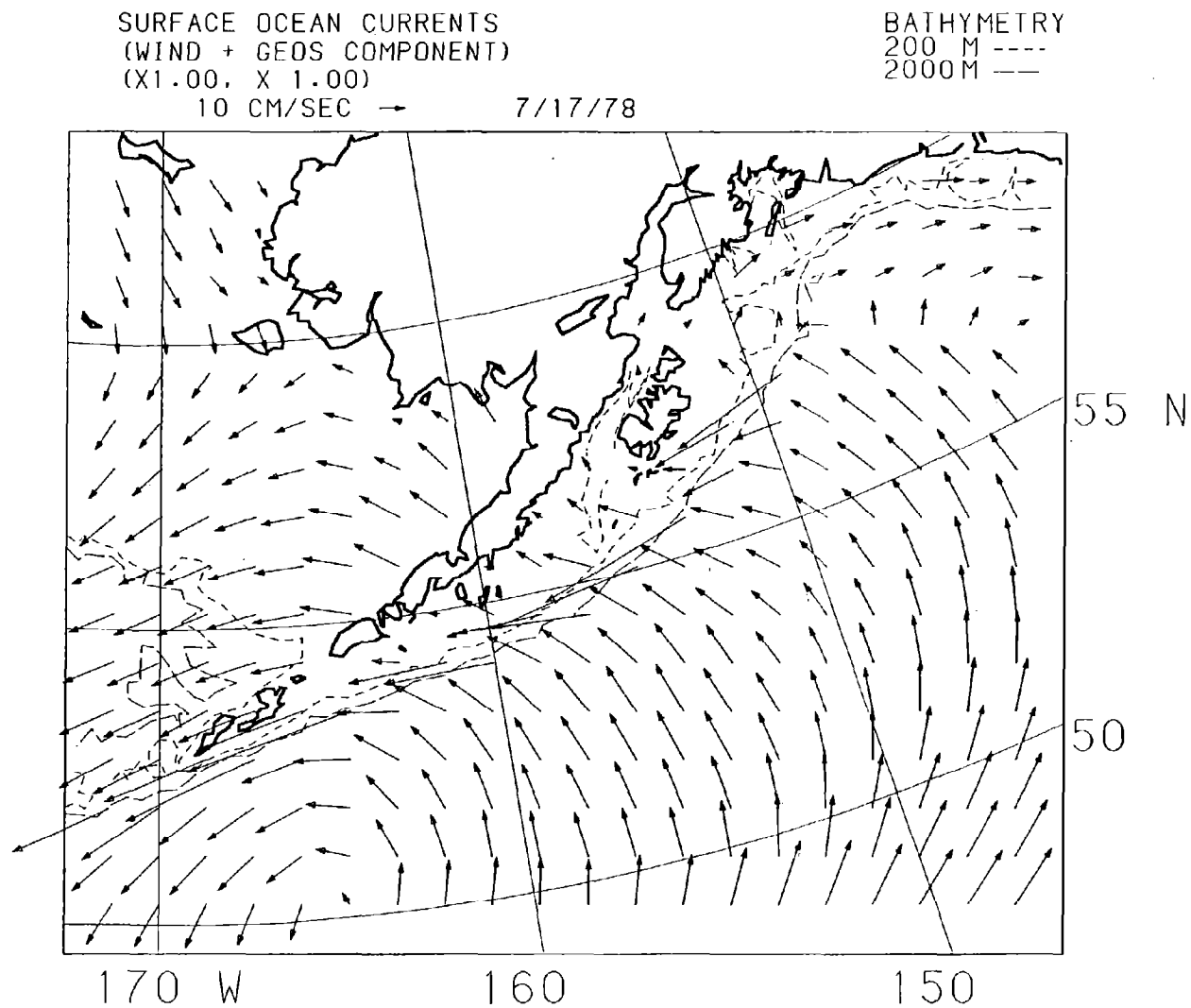


Figure 6. --Total surface ocean current vector field (cm/sec) computed by OSCURS model (sum of geostrophic plus wind current) for 17 July 1978 (model output).

rest of the grid are between 10 and 20 cm/sec. Current patterns will, therefore, be considerably variable day to day and season to season due to the brevity and variability of the winds. Rather than show the 15,330 possible daily examples of total current fields between 1946 and 1987, we have selected several days or months of current, fields and analyzed their cumulative effect on drift.

Progressive Displacement Vectors

In order to show this cumulative effect, the model calculates a series of daily displacement vectors and stores their coordinates in a file for later plotting as progressive vector tracks. The model requires only a list of starting locations in grid units for each desired track, a start date, and a stop date. For each day, the model interpolates a velocity vector within the total current field at the location of each start point, then calculates the displacement for 24 hours of drift at that velocity, and stores the start and end points in a file. The end points are used as the start points for the next day's computations. The loop continues in daily time steps until the model reaches the stop date, which ends the model run. The graphics output program then reads the file of daily start and end points, connects the points to form the progressive vector tracks, and plots a background chart with the square model grid, coastline, and bathymetry.

In this section we will compare the tracks computed by the original model and the drifter tracks deployed at the same

starting point in the ocean. We are fortunate to have obtained the data for location versus time from the first set of three drifters tracked by satellite navigation in the western Gulf of Alaska from 17 July 1978 to 1 January 1979 (Reed 1980). As we shift our presentation from gridded fields of velocity vectors to spatial displacements over time, we can examine drift conditions anywhere within the grid. We will discuss the geostrophic and wind drift components of flow separately from the new, Lagrangian viewpoint before we examine how well the original model computations agree with these drifter tracks.

Geostrophic Current

Geostrophic currents occur along streamlines which are independent of time. Therefore, the model may be started from a given location on any date and the flow will trace the same track. Figure 7(a) shows the drift displacement caused only by geostrophic flow.

The same features seen in the vector field presentation of geostrophic flow (Fig. 2) are also seen in this progressive vector representation (Fig. 7(a)). On the shoreward side of the oblong Gulf of Alaska Gyre, flow conditions are unrealistically slow in the Alaskan Stream until the amplifying factor is added (Fig. 7(b)). Maximum geostrophic flow occurs near and along the 2,000 m depth contour. Here, the surface water takes about 3 months (mid-July to early November) to get from Kodiak Island to Unimak Pass, but with the amplifier this geostrophic drift moves the same distance in about 1 month (mid-July to mid-August). The

DAILY PROGRESSIVE VECTORS
FROM 7/17/78
TO 12/31/78

OCEAN CURRENTS
(WIND = 0.0)
(GEOSTROPHIC = 1.0)

BATHYMETRY
200 M - - - -
2000M - - - -

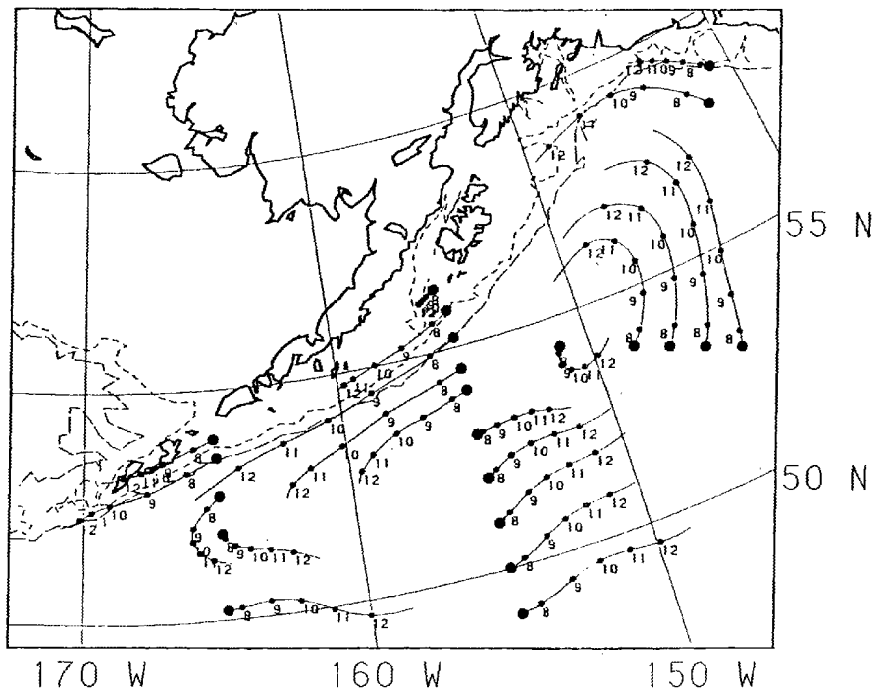


Figure 7(a).--Progressive daily transport vectors. Distance of surface water movement due to geostrophic current component only from 17 July to 31 December 1978. The first day of each month is numbered along the tracks (i.e., August = 8, September = 9, etc.).

DAILY PROGRESSIVE VECTORS
FROM 7/17/78
TO 12/31/78

OCEAN CURRENTS
(WIND = 0.0)
(GEOSTROPHIC = 1.0)

BATHYMETRY
200 M - - - -
2000 M - - - -

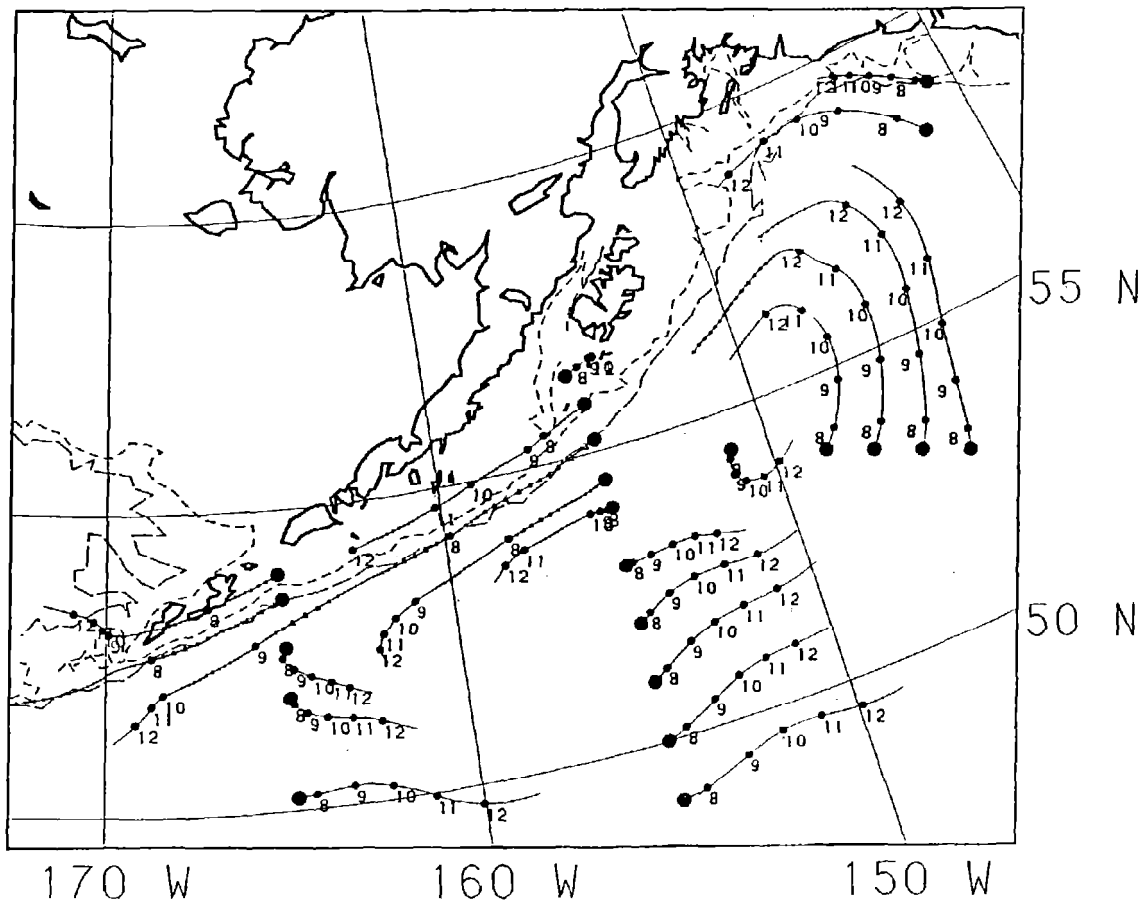


Figure 7(b). --Progressive daily transport vectors. Distance of surface water movement due to geostrophic current component only from 17 July to 31 December 1978. This shows effect of model enhancement factors in the Alaskan Stream near the 2,000 m depth contour compared to Figure 7(a).

advantage of progressive vector plots over plots of velocity vector fields is that the progressive vector plots give the viewer a good estimate of net distance drifted over any convenient time interval (transport). These charts have a practical application in finding the rate of transport of flotsam (for example, fish eggs and larvae or marine debris such as derelict nets or garbage). The asymmetry of drift speeds in the Gulf of Alaska Gyre appears to be greater than an order of magnitude. In the narrow Alaskan Stream, a planktonic object may be swept out of the area of interest within 1 to 2 months, whereas the offshore return circuit around the Gyre, due only to geostrophic flow, appears quite lengthy at about 2 years. Complexity of flow increases dramatically, however, with the addition of wind effects.

Wind Drift

By isolating the effects of wind on the flow regime, we show that the wind component of surface drift displacement (Fig. 8) generally increases offshore and toward the southeast. Short-term variability is pronounced and depends upon both location within the grid and time scales of up to 2 weeks. Time scales greater than 1 month, however, show well-developed displacement trends. Eastward wind drift along lat. 50°N and northerly drift into the head of the gulf move in the same direction as the geostrophic flow, but the eastward to northeastward trending wind drift over the continental terrace clearly opposes the strong, narrow, southwestward geostrophic

DAILY PROGRESSIVE VECTORS

FROM 7/17/78

TO 12/31/78

OCEAN CURRENTS

(WIND = 1.0)

(GEOSTROPHIC = 0.0)

BATHYMETRY

200 M - - - -

2000M - - - -

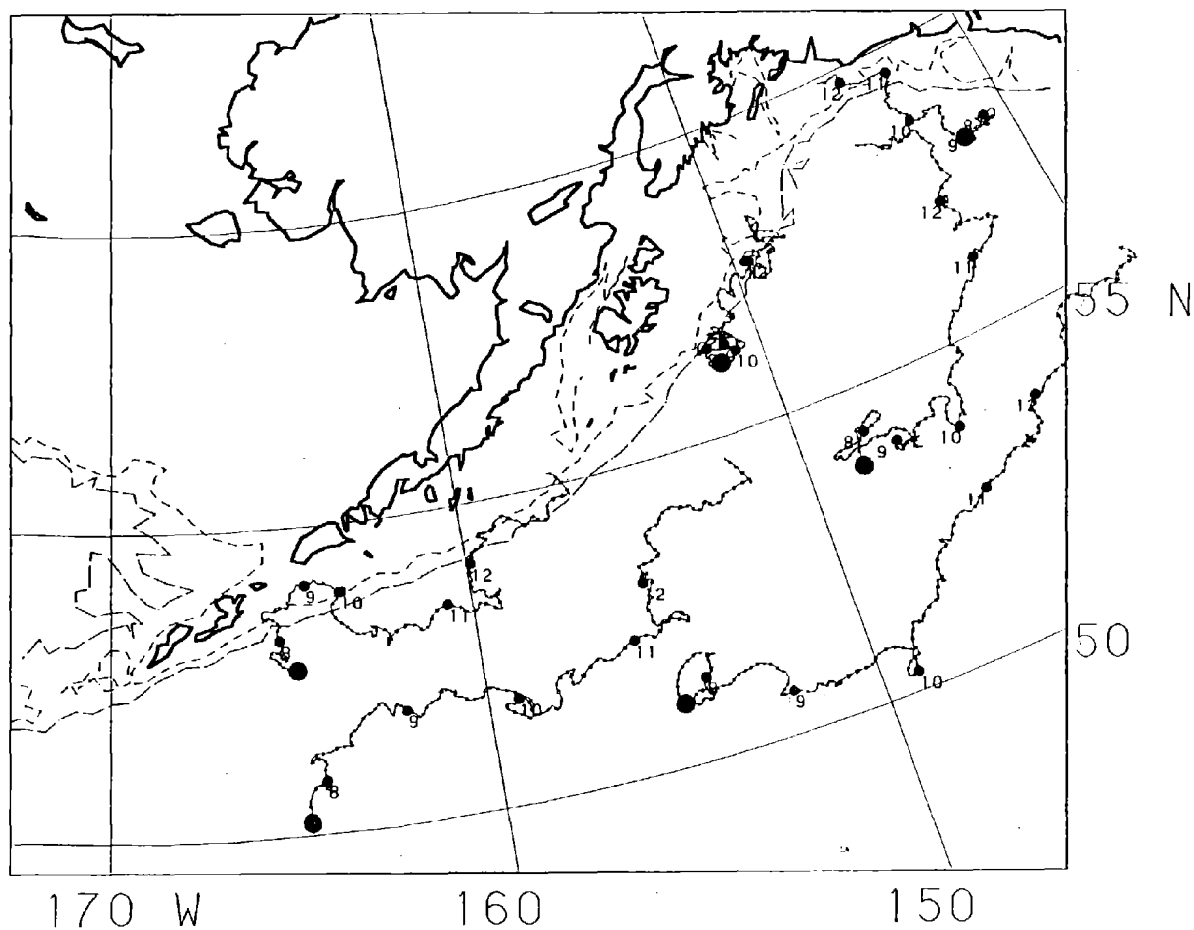


Figure 8.--Progressive daily transport vectors. Distance of surface water movement due only to wind current component from 17 July to 31 December 1978.

flow in the Alaskan Stream. The tendency of the wind to force the surface water offshore increases toward the west. This supports the theory that the water recirculates. The magnitude of net wind drift is weakest near Kodiak Island and strongest offshore, where it more than doubles the geostrophic component. Embedded within these dominant features are mesoscale oscillatory features. Although there is considerable meandering, the easterly drift has few closed eddies. On the other hand, the wind drift near Kodiak Island appears to be composed mostly of eddies or tight meanders with very little net northerly drift. We merged these two components- as vector sums to obtain total drift tracks..

Total Drift Versus Drifter Data

Although the merged tracks displayed some of the characteristics of the original geostrophic and wind current components described separately above, the characteristics of the resultant tracks were more unpredictable than expected. Using the same starting points as the component model runs, the 1988 version of the model calculated total surface current (Fig. 9). These calculations clearly show the gyral nature of the overall flow in the gulf. The strong southwestward geostrophic component dominates the flow in the Alaskan Stream despite the opposing wind, and the wind features dominate the eastward drift in the offshore branch of the gyre. Of great concern was the small circuit in the recirculation of the track started in the Alaskan Stream. This track turned offshore near long. 162°W as expected

DAILY PROGRESSIVE VECTORS

FROM 7/17/78

TO 12/31/78

OCEAN CURRENTS

(WIND = 1.0)

(GEOSTROPHIC = 1.0)

BATHYMETRY

200 M ----

2000M ---

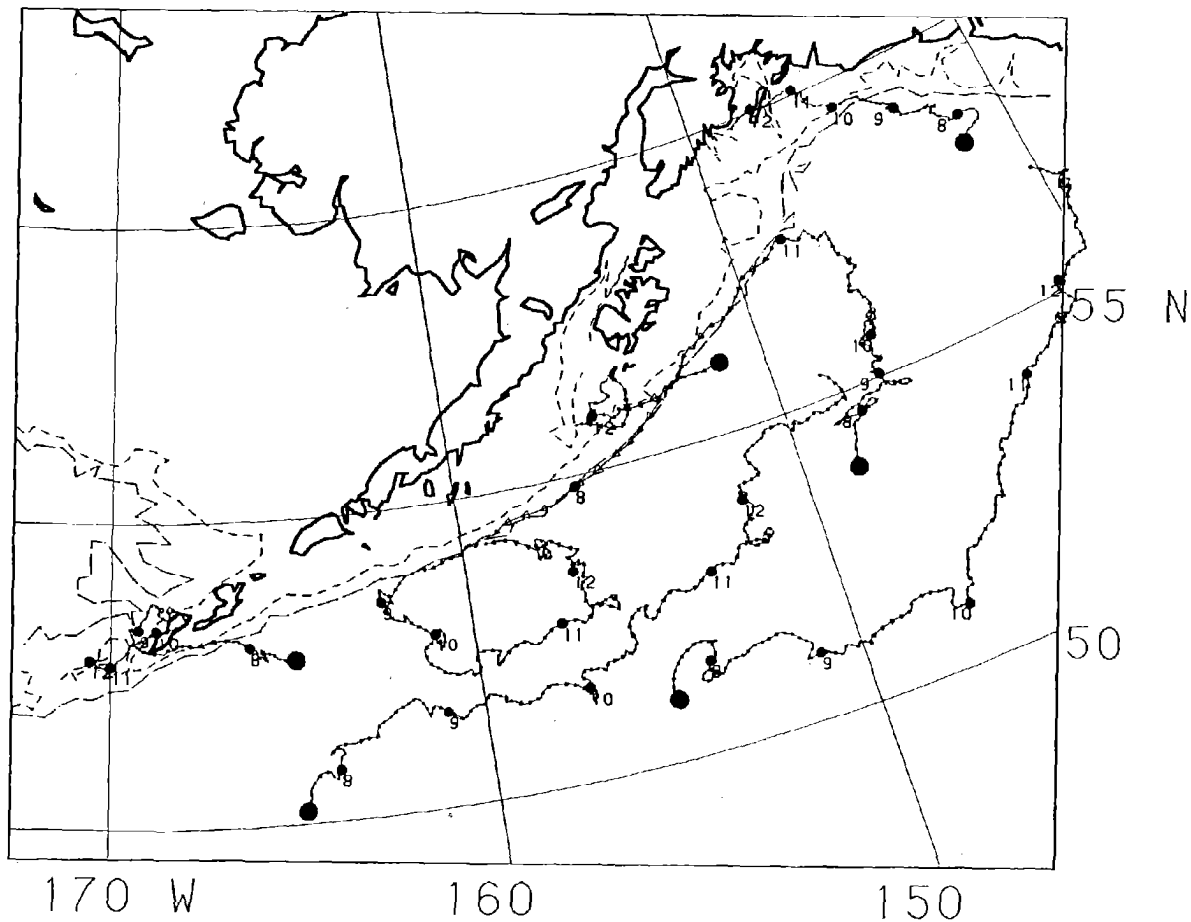


Figure 9.--Progressive daily transport vectors. Distance of surface water movement due to daily total currents from 17 July to 31 December 1978.

then proceeded eastward only to long. 156°W before turning to rejoin the stream without making a full circuit around the gyre. Our concerns were amplified when model tracks were compared to actual drifter data.

Disparities were not unexpected between the original model simulations and the drifters started in the Alaskan Stream southeast of Kodiak Island. The narrow, strong shear flow of the Alaskan Stream was obviously a poor place to start a model simulation with a grid this coarse. Even the ground-truth measurements with the three drifters (which were released very close together (9 km)) showed a wide dispersion over a five-month drift (Fig. 10) (Reed 1980). Although the model run that started at the initial release point did not show much promise as a drifter track simulator (Fig. 11), certain features of our component analysis above revealed potential similarities and further investigation did lead to some positive visual correlations. When runs were started downstream at locations outside the Alaskan Stream, each of the three drifter tracks (Figs. 12, 13, and 14) showed much closer agreement. We examined alternative empirical functions for computing drift and used linear tuning of equations to reach a final best-fit version of the model which could be used in other locations or for variability studies,

DAILY PROGRESSIVE VECTORS
FROM 7/17/78
TO 12/31/78

OCEAN CURRENTS
(WIND = 1.0)
(GEOSTROPHIC = 1.0)

BATHYMETRY
200 M - - - -
2000 M - - - -

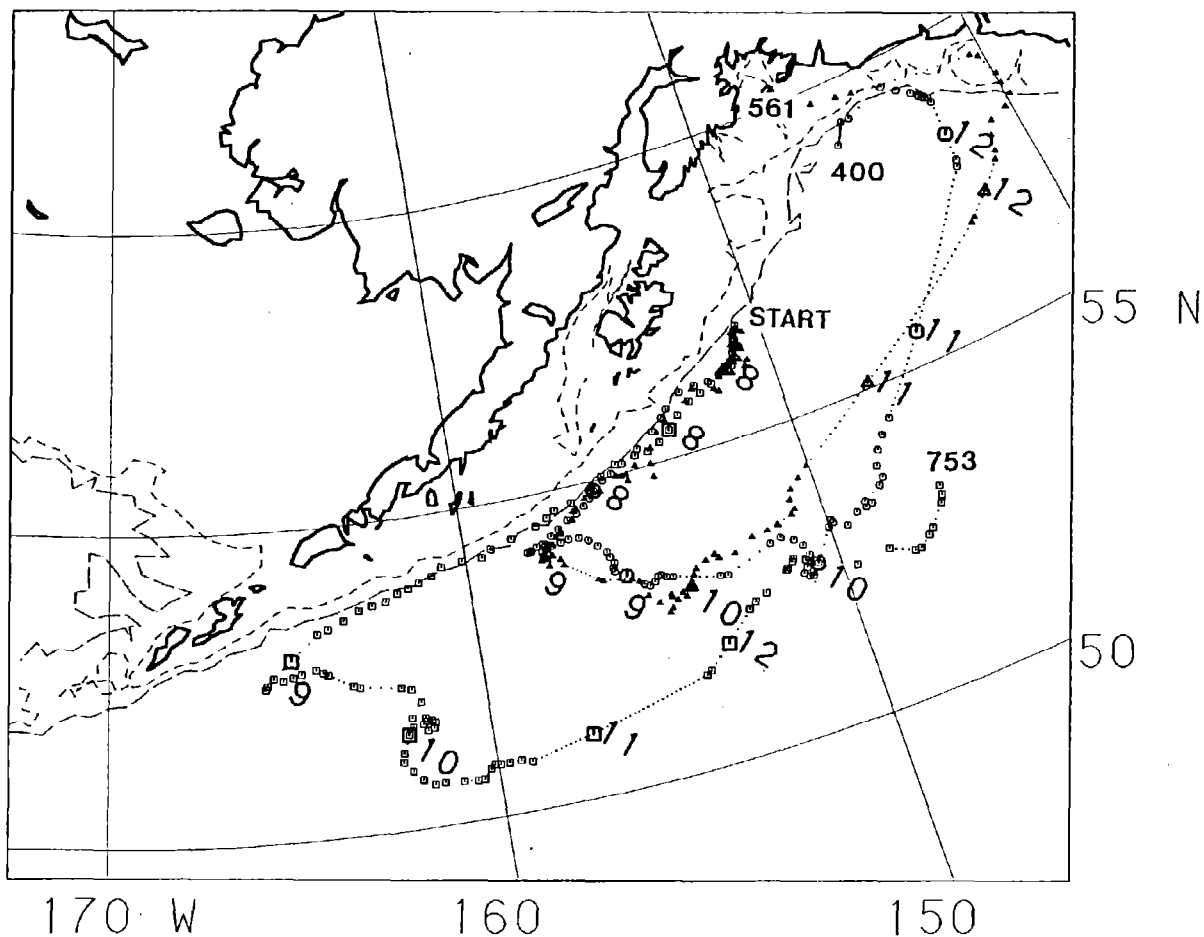


Figure 10. --Daily (0000Z) locations of three satellite tracked drifters released close together in the Alaskan Stream on 17 July 1978. Small dots indicate linear estimate of daily position where gaps exist in the data (Reed 1980).

DAILY PROGRESSIVE VECTORS
FROM 7/17/78
TO 12/31/78

OCEAN CURRENTS
(WIND = 1.0)
(GEOSTROPHIC = 1.0)

BATHYMETRY
200 M - - -
2000M ---

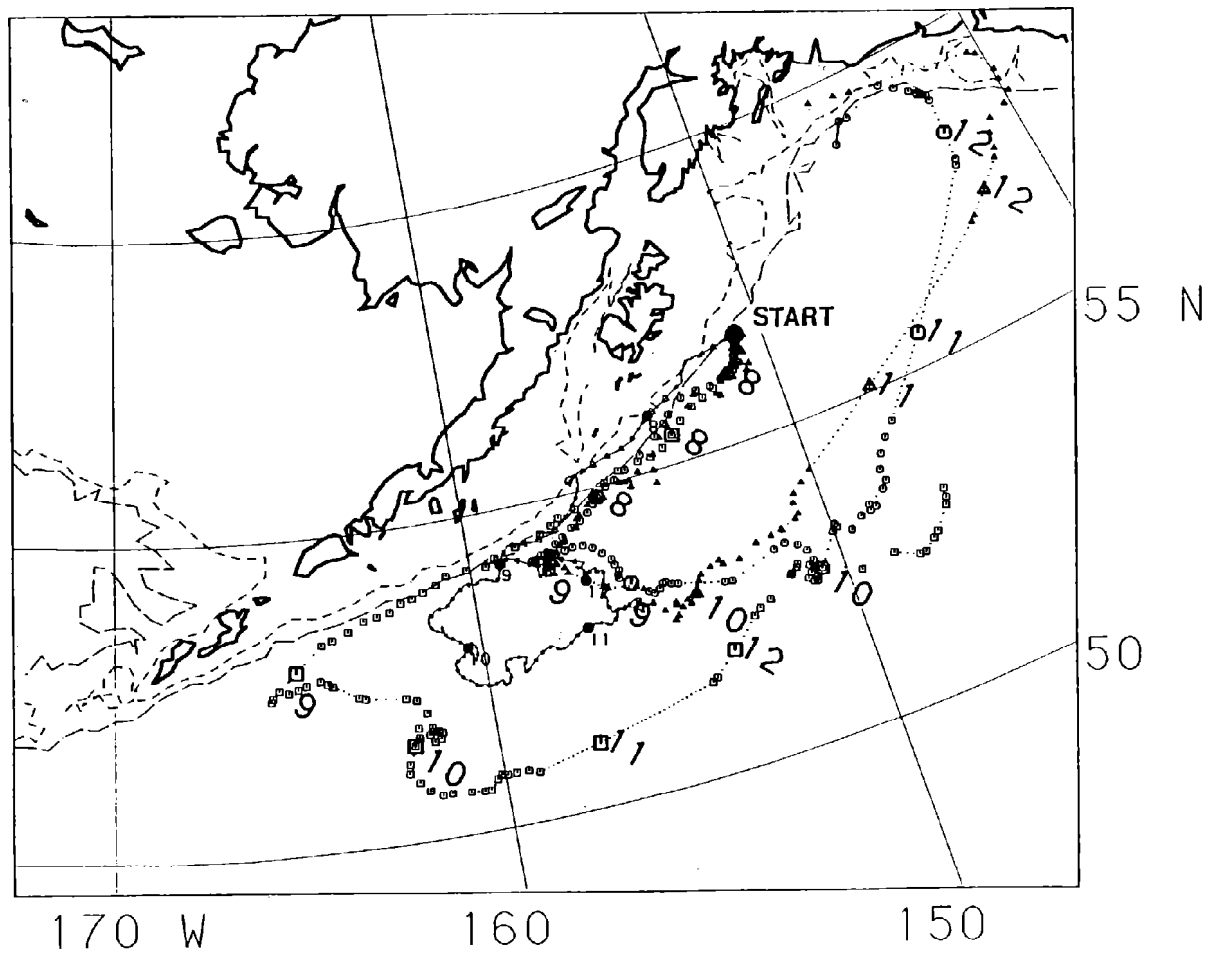


Figure 11. --Daily progressive vector track computed by original (1988) OSCURS model from starting point of 17 July. Compare tracks of three drifters released near the same starting point on the same day.

DAILY PROGRESSIVE VECTORS

FROM 9/21/78

TO 12/31/78

OCEAN CURRENTS

(WIND = 1.0)

(GEOSTROPHIC = 1.0)

BATHYMETRY

200 M ----

2000M ---

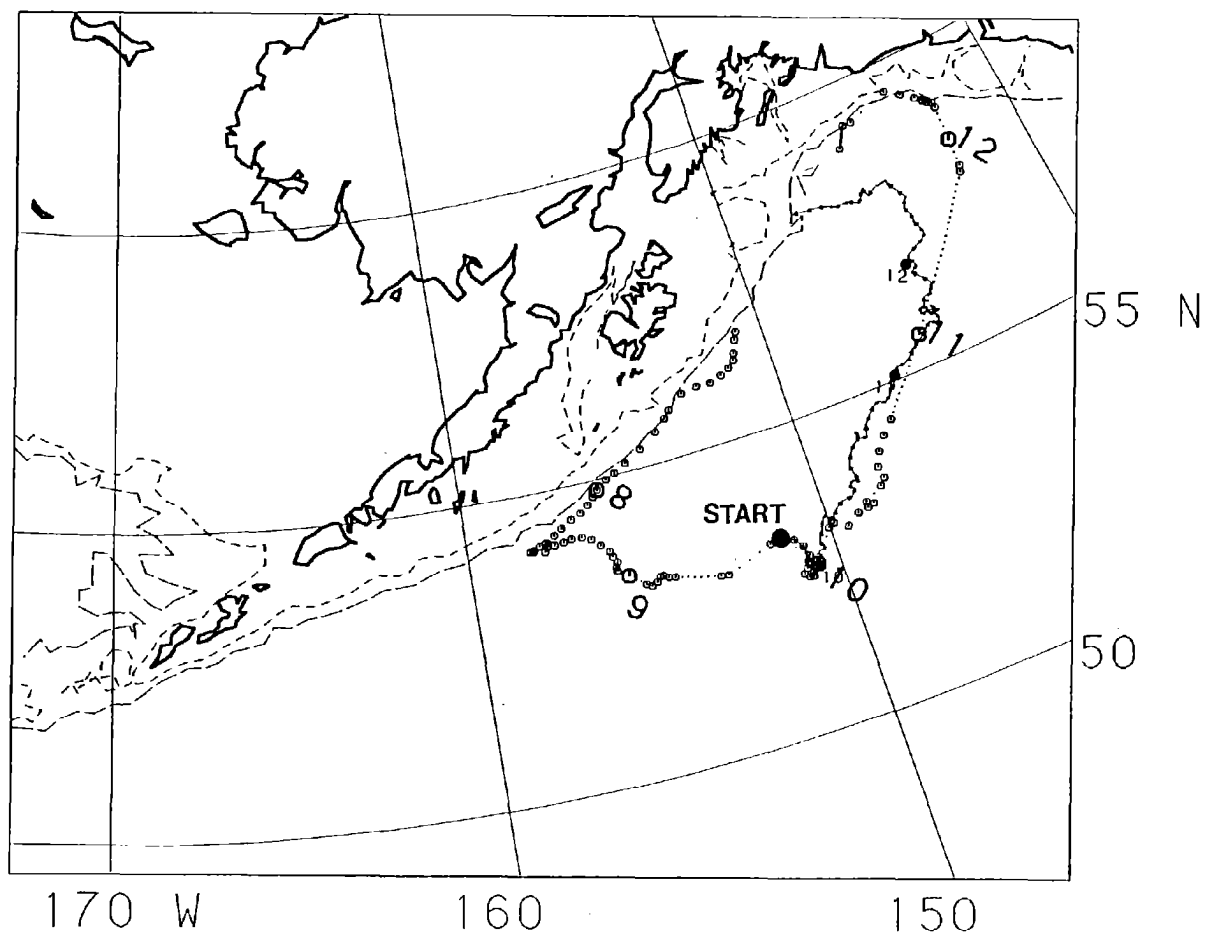


Figure 12.--Daily progressive vector track computed by the original (1988) OSCURS from the downstream starting point of 21 September on the track of drifter No. 400.

DAILY PROGRESSIVE VECTORS
FROM 9/21/78
TO 12/31/78

OCEAN CURRENTS
(WIND = 1.0)
(GEOSTROPHIC = 1.0)

BATHYMETRY
200 M - - - -
2000M - - - -

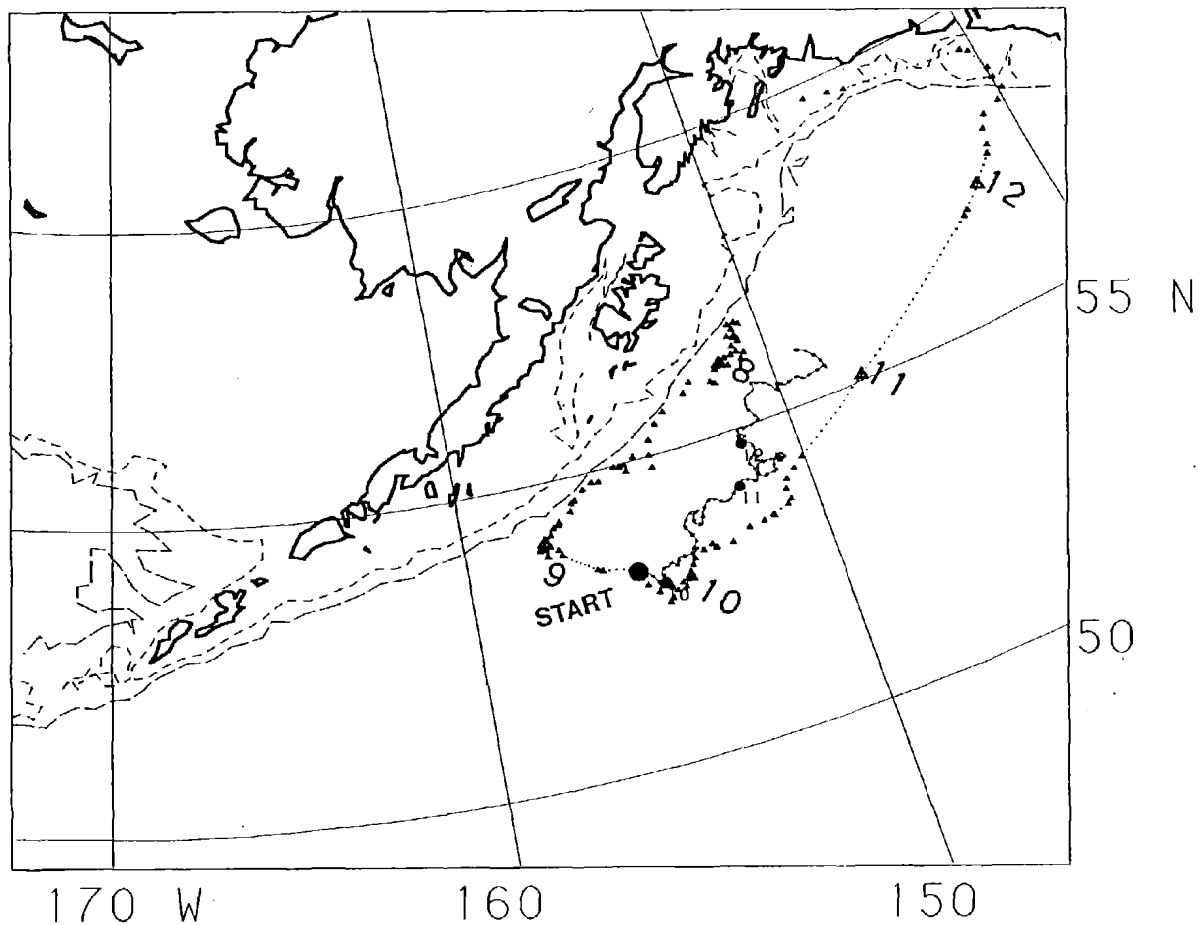


Figure 13.--Daily progressive vector track computed by the original (1988) OSCURS from the downstream starting point of 21 September on the track of drifter No. 561.

DAILY PROGRESSIVE VECTORS

FROM 9/21/78

TO 12/31/78

OCEAN CURRENTS

(WIND = 1.0)

(GEOSTROPHIC = 1.0)

BATHYMETRY

200 M - - - -

2000M - - - -

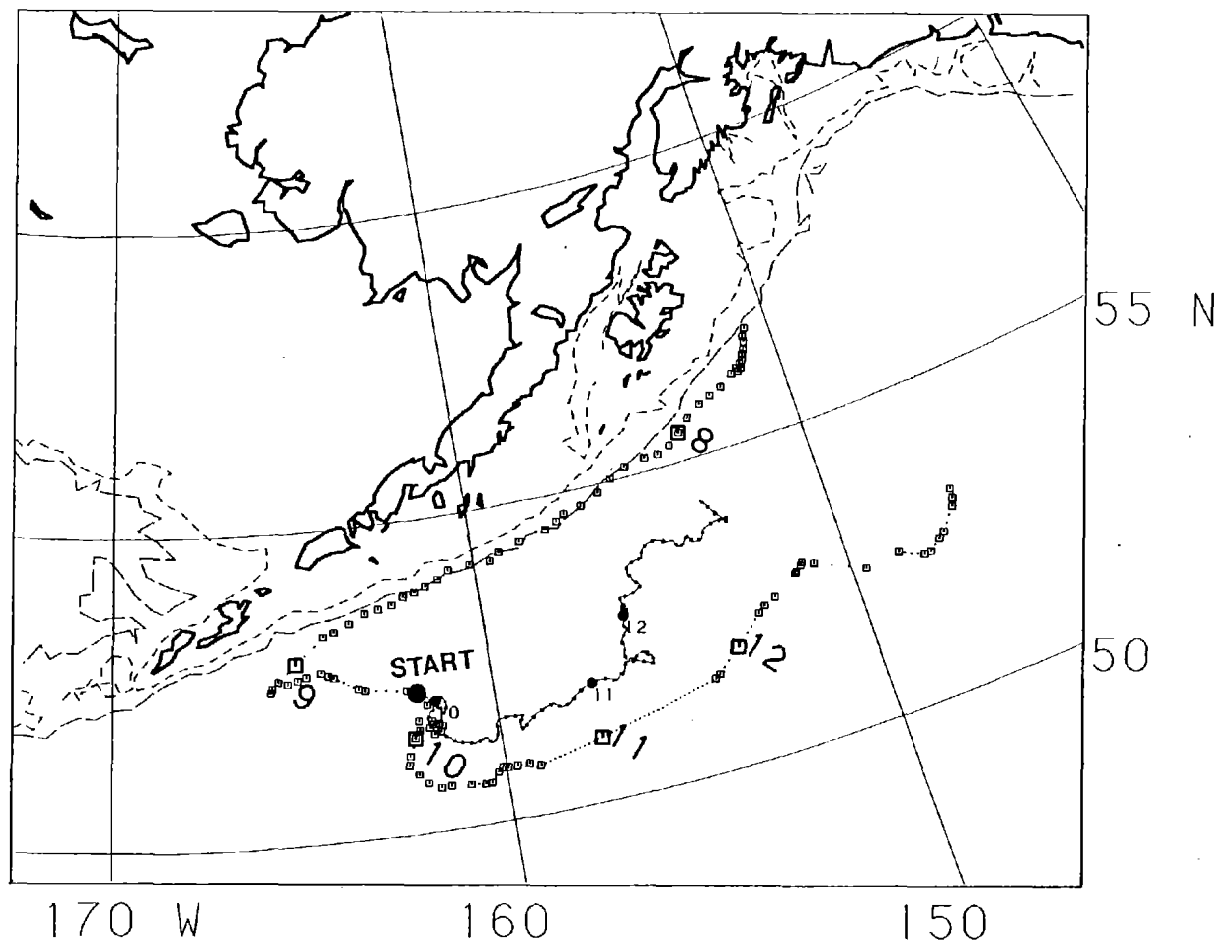


Figure 14.--Daily progressive vector track computed by the original (1988) OSCURS from the downstream starting point of 21 September on the track of drifter No. 753.

REASSESSMENT OF DRIFT CALCULATIONS

At this stage of development, the model's agreement with drifter tracks was mostly subjective. Although there were obvious deficiencies in the original 1988 version, visual patterns in the offshore portion of the tracks indicated some promising clues for enhancing this agreement using other empirical relationships or best-fit tuning factors. Discrepancies may arise through the computations of either wind or currents, but we preferred to leave the established wind computations (Larson 1975) unaltered and concentrate on evaluating the effects of various other empirical equations for calculating current speed and the angle of deflection to the right of the wind. We also show the sensitivity of computed tracks to speed or angle by varying the tuning factors one at a time.

Speed of Drift Driven by Wind Speed

A summary of numerous empirical formulae for calculating drift currents from field and laboratory data (Huang 1979) shows the complexity of the problem of calculating an ocean current from a given wind. Although speed and angle of deflection are weakly related, we will first discuss speed alone. We used three selected functions to calculate drift speeds (Fig. 15): 3.5% of the wind speed for an oilspill trajectory analysis model (Samuels, et al. 1982), 1.5% of the wind speed from comparisons with satellite drifters tracked in midlatitude (McNally 1981),

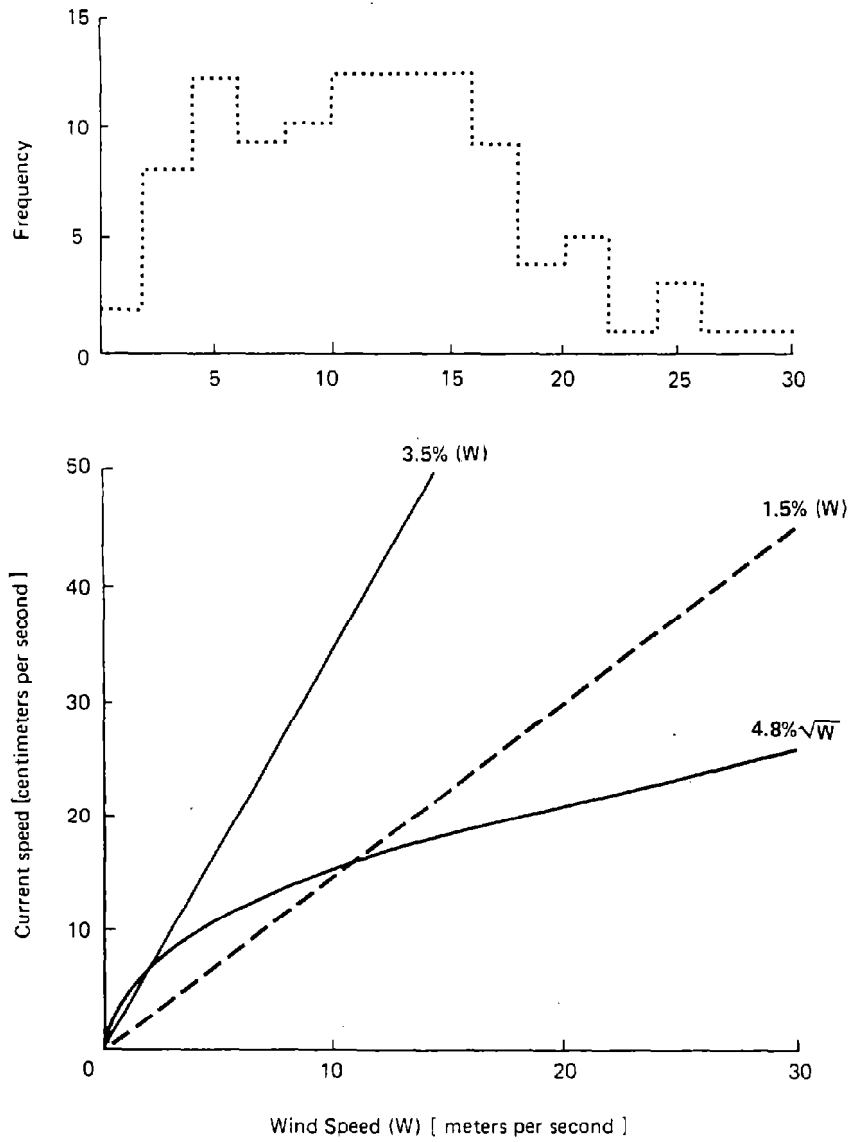


Figure 15. --Three empirical functions for computing ocean current speed (cm/sec) from wind speed (m/sec) and average wind frequencies in 2 m/sec bins along offshore portion of three drifter tracks (last 100 days).

and 4.8 times the square root of the wind speed (Witting 1909; Hubert and Laevastu 1965; Ingraham and Miyahara 1988). Computed current speeds will be quite different depending upon which function is used and the local winds. Wind frequencies (upper part of Fig. 15) show that the 0000Z wind speeds from 4 to 16 m/sec were encountered most often along the offshore portion of these drifter tracks from July through December 1978. All three functions give similar currents at low wind speeds of a few meters per second but diverge rapidly at greater wind speeds. Samuels et al.'s (1982) 3.5% will give unrealistically strong currents at wind speeds greater than 15 m/sec; McNally's (1981) 1.5% appears to have an intermediate effect; and Witting's (1909) square root function appears the weakest in overall magnitude but favorable in that it takes into account frictional effects which would dampen the otherwise linear increase in current at higher wind speeds. In terms of percent of the wind speed, the Witting formula takes on the characteristics of both the other functions: at low wind speeds up to about 3 m/sec it is equivalent to the formula of Samuels et al. (3.5%); it decreases to McNally's formula (1.5%) near 10 m/sec and finally drops below 1% at wind speeds beyond 24 m/sec.

We started model runs using these three functions at selected dates along each drifter track to find areas of agreement and to show the isolated effect of speed changes on model-generated tracks. Because of the large space divergences between the three measured drifter tracks (Nos. 400, 561, and 753), we will consider portions of each track separately.

Drifter No. 400 started on 17 July (Fig. 16). The original Witting (run No. 1) and 1.5% (run No. 2) tracks were nearly identical, slow with no significant offshore recirculation, but the 3.5% track (run No. 3) showed more discernible features of the offshore flow despite the excessive speed. Runs Nos. 1 and 2 from 13 August near lat. 54°N , long. 158°W where the drifter track started to move offshore out of the Alaskan Stream (Fig. 17) both showed restricted, minirecirculation, but the recirculation of run No. 3 nearly matched the shape of the drifter's 14-day meander near 1 October. The speeds derived from the 3.5% function were obviously too high: the distance tracked by this function from 1 October to 1 November was twice that traveled by the drifter. Offshore model runs from 21 September near lat. 53°N , long. 151°W in the eastward drift (Fig. 18a) showed much better agreement compared to the inshore model runs, as did the 21 September runs for drifter No. 561 (Fig. 18b) and drifter No. 753 (Fig. 18c).

We concluded that the Witting formula of the original model was too slow and the function of Samuels et al. (3.5%) was too fast. An intermediate function would be best for calculating speed, perhaps a linear tuning multiplier times the Witting formula. A consistent feature in the model-drifter mismatch was the tendency for all the above model tracks to stay to the left of the drifter. Therefore, we went back to our Witting speed function and computed a similar sequence of model tracks varying the angle of deflection.

DAILY PROGRESSIVE VECTORS

FROM 7/17/78

TO 12/31/78

OCEAN CURRENTS

(WIND = 1.0)

(GEOSTROPHIC = 1.0)

BATHYMETRY

200 M - - - -

2000 M - - - -

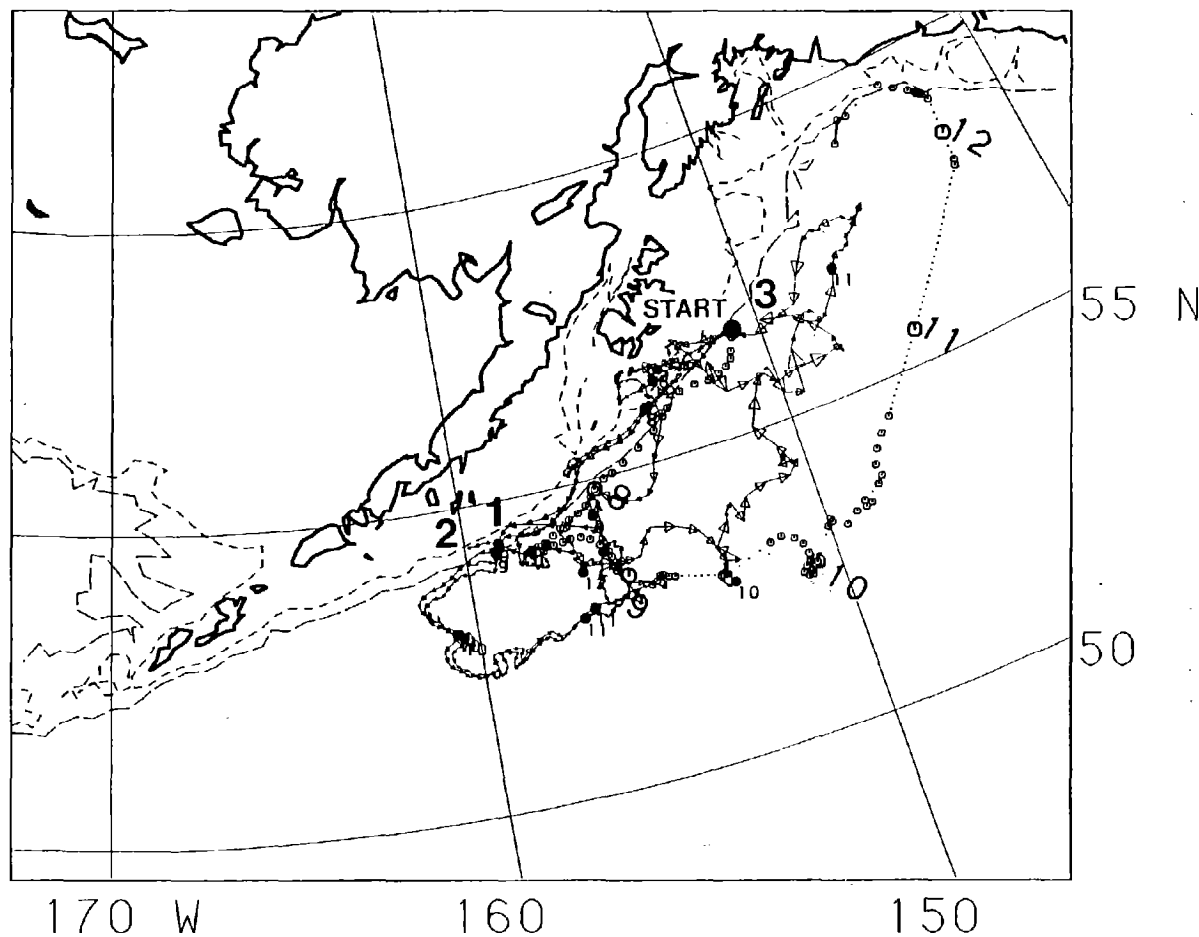


Figure 16.--Three daily progressive vector tracks started at the group release location of drifters No. 400, 561, and 753 on 17 July. Three speed functions are compared; run No. 1 (Witting), run No. 2 (1.5%), and run No. 3 (3.5%).

DAILY PROGRESSIVE VECTORS
FROM 8/13/78
TO 12/31/78

OCEAN CURRENTS
(WIND = 1.0)
(GEOSTROPHIC = 1.0)

BATHYMETRY
200 M - - - -
2000 M - - - -

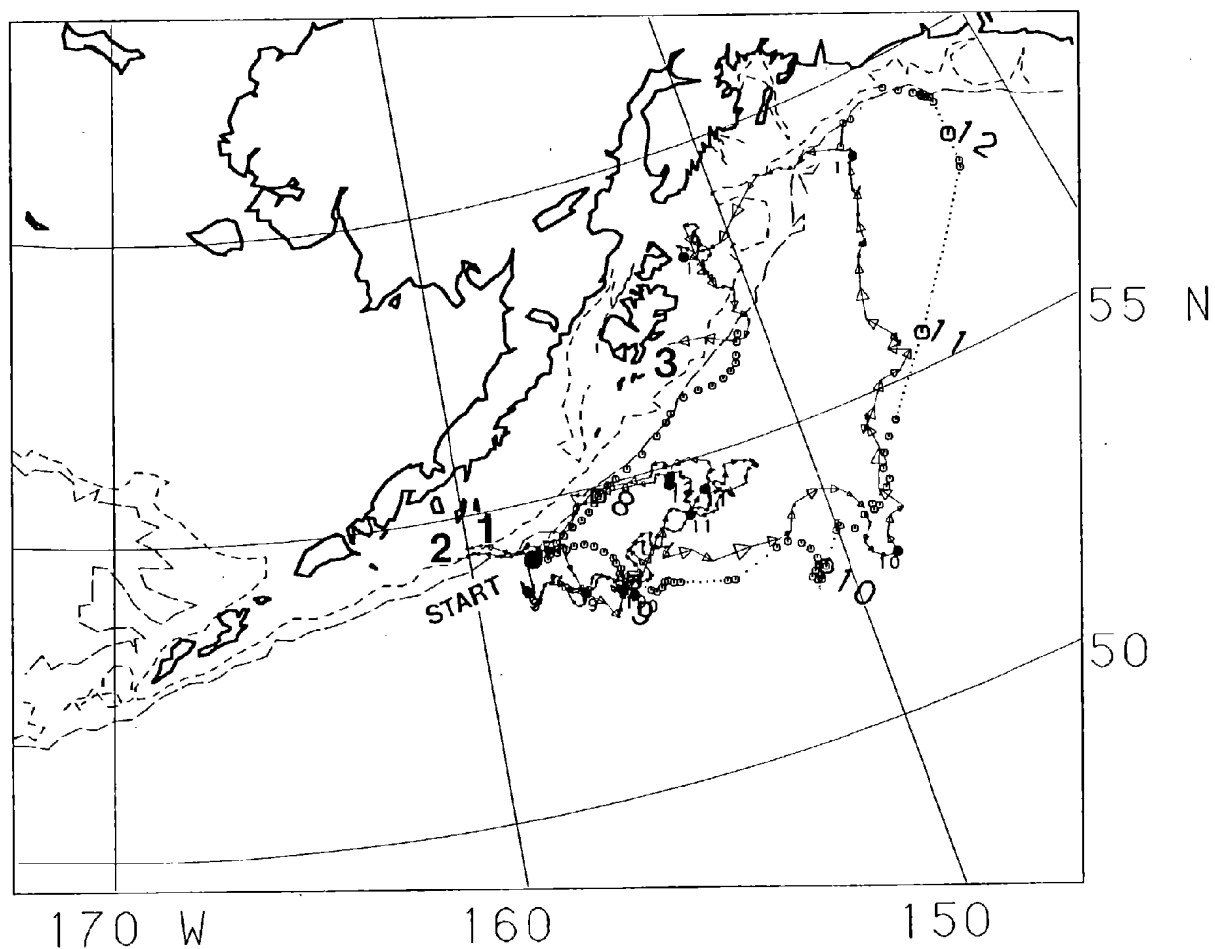


Figure 17.--Three daily progressive vector tracks started at the location of drifter No. 400 on 13 August. The same three speed functions (Fig. 16) are compared for runs started down stream at the beginning of recirculation.

DAILY PROGRESSIVE VECTORS
FROM 9/21/78
TO 12/31/78

OCEAN CURRENTS
(WIND = 1.0)
(GEOSTROPHIC = 1.0)

BATHYMETRY
200 M - - - -
2000 M - - - -

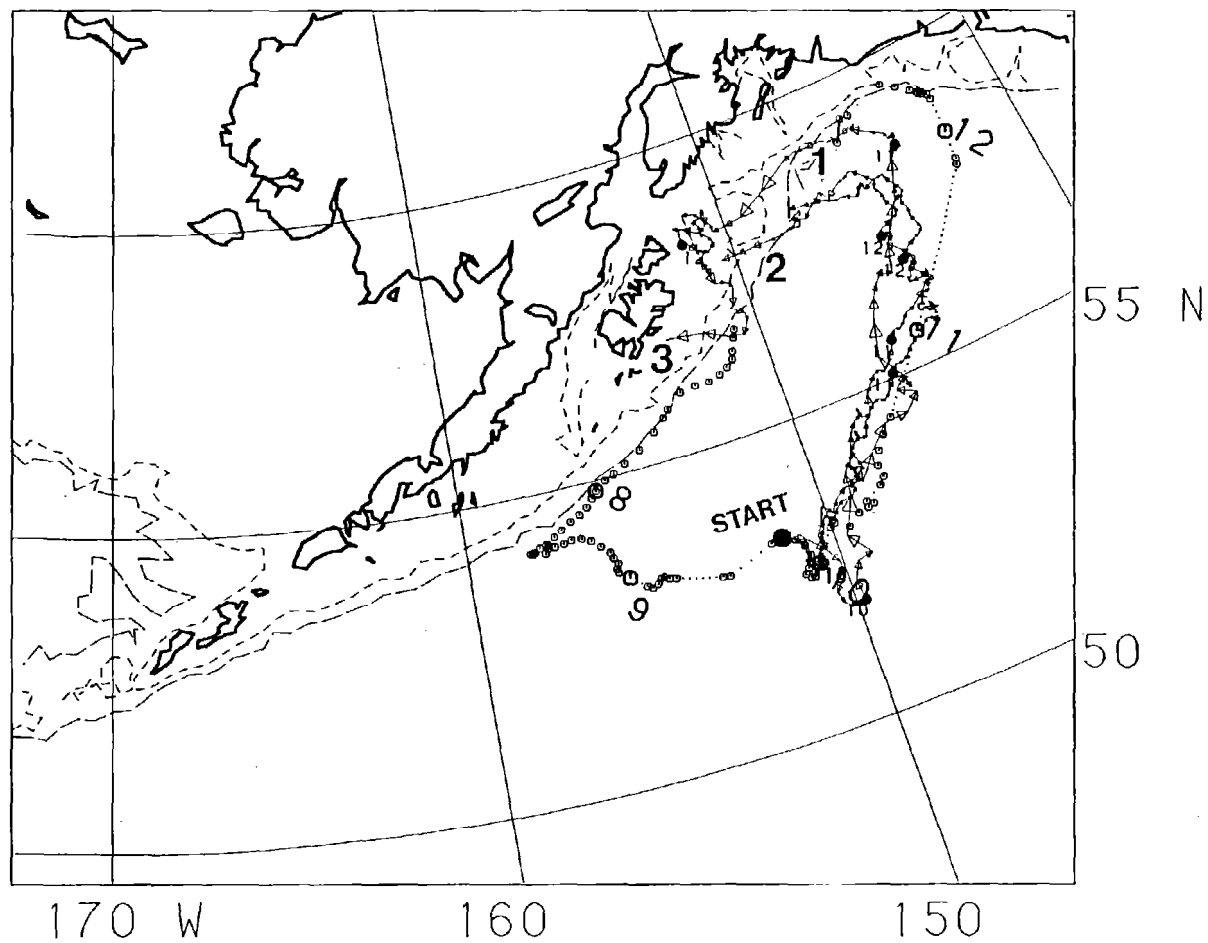


Figure 18(a). --Three daily progressive vector tracks started at the location of drifter No. 400 on 21 September. Three speed functions are compared in offshore water; run No. 1 (Witting, run No. 2 (1.5%), and run No. 3 (3.5%).

DAILY PROGRESSIVE VECTORS

FROM 9/21/78

TO 12/31/78

OCEAN CURRENTS

(WIND = 1.0)

(GEOSTROPHIC = 1.0)

BATHYMETRY

200 M ----

2000M ---

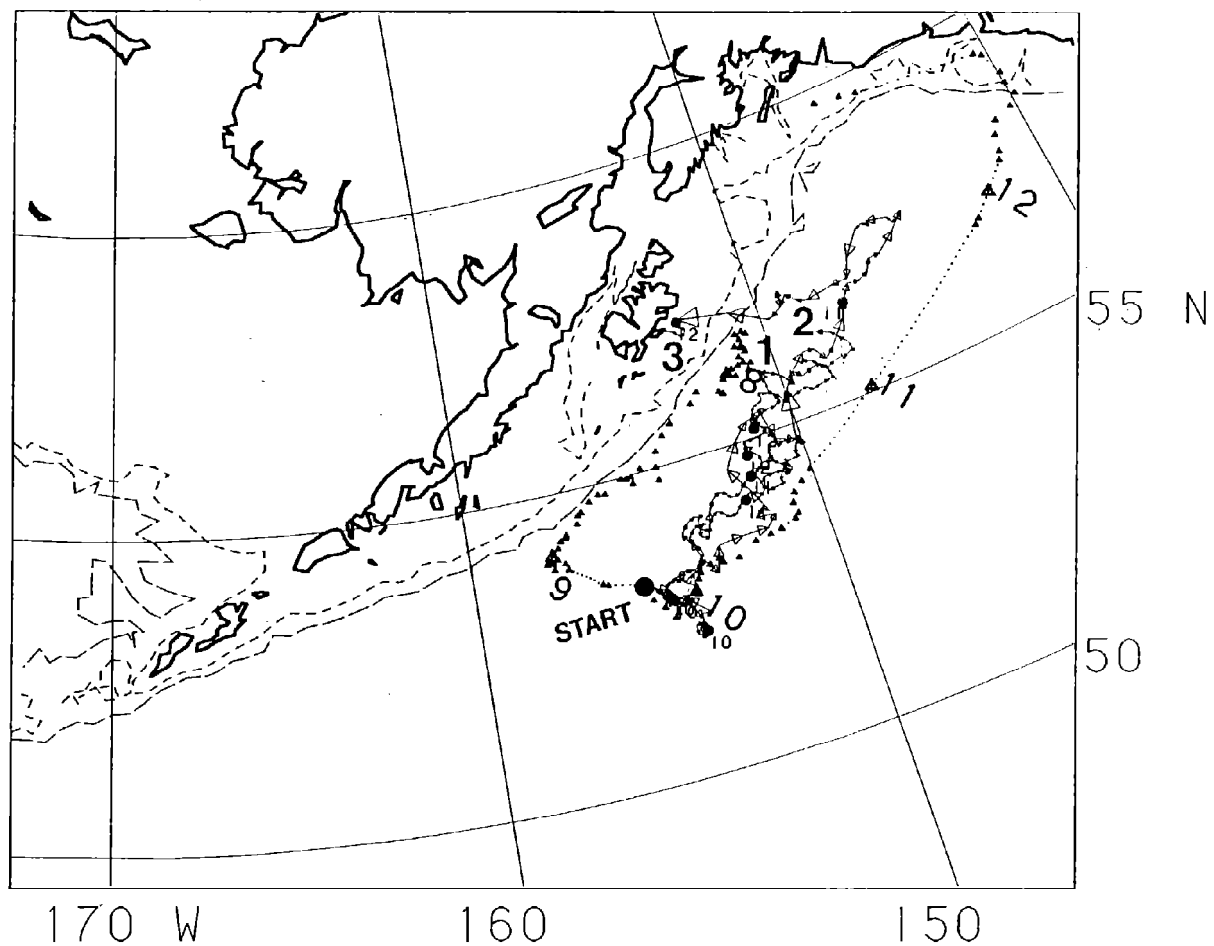


Figure 18(b) .--Three daily progressive vector tracks started at the location of drifter No. 561 on 21 September. Three speed functions are compared in offshore water; run No. 1 (Witting), run No. 2, (1.5%), and run No. 3 (3.5%).

DAILY PROGRESSIVE VECTORS

FROM 9/21/78
TO 12/31/78

OCEAN CURRENTS

(WIND = 1.0)
(GEOSTROPHIC = 1.0)

BATHYMETRY

200 M - - - -
2000 M - - - -

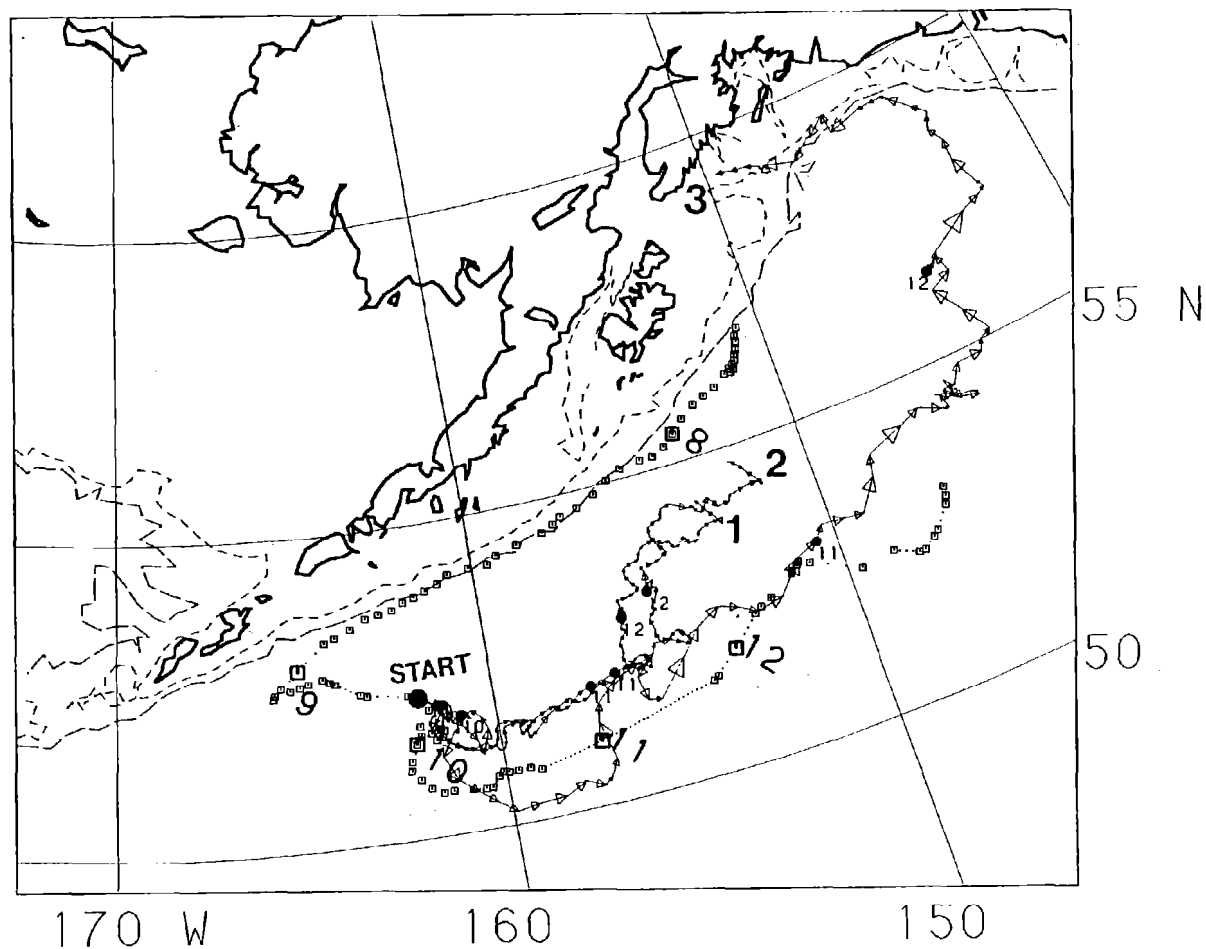


Figure 18(c).--Three daily progressive vector tracks started at the location of drifter No. 753 on 21 September. Three speed functions are compared in offshore water; run No. 1 (Witting), run No. 2 (1.5%), run No. 3 (3.5%).

Clockwise Angle of Deflection

There is still conflict of opinion over which function best computes the angle of deflection of surface drift to the right of the wind vector (Amstutz and Samuels 1984). Most studies (Samuels. et al. 1982; Neumann 1939) indicate that the angle decreases with increasing wind speed (Fig. 19), as does our choice of the Witting function for the 1988 OSCURS. Weber (1983), however, reports an increasing function which varies from 23 degrees at a low wind speed of 5 m/sec to 30 degrees at a high wind speed of 30 m/sec, further complicating the issue. Figure 19 summarizes this dispute by giving a visual comparison of the functions (Amstutz and Samuels 1984), but McNally (1981) presents some support for larger angles of deflection in a comparison of wind and ocean drifter movements, indicating an angle of deflection of 20-30 degrees for wind speeds from 2 m/sec up to about 10 m/sec. As in the above discussion of speed only, the wind frequencies shown near the bottom of Figure 19 (dotted line) indicate that about half of the time (for winds greater than 11 m/sec) angles of deflection computed by the witting formula in our original model were relatively small, less than 10 degrees. We chose three functions to show the sensitivity of the computed tracks to angle of deflection: 1) Witting, 2) a constant 20 degrees, and 3) a constant 30 degrees.

For drifter No. 400 with a 17 July starting date (fig. 20) the recirculation feature opened up nicely when a constant 20 or 30 degree clockwise deflection angle was used in runs No. 2 and No. 3, respectively: but the overshoot of the model tracks past

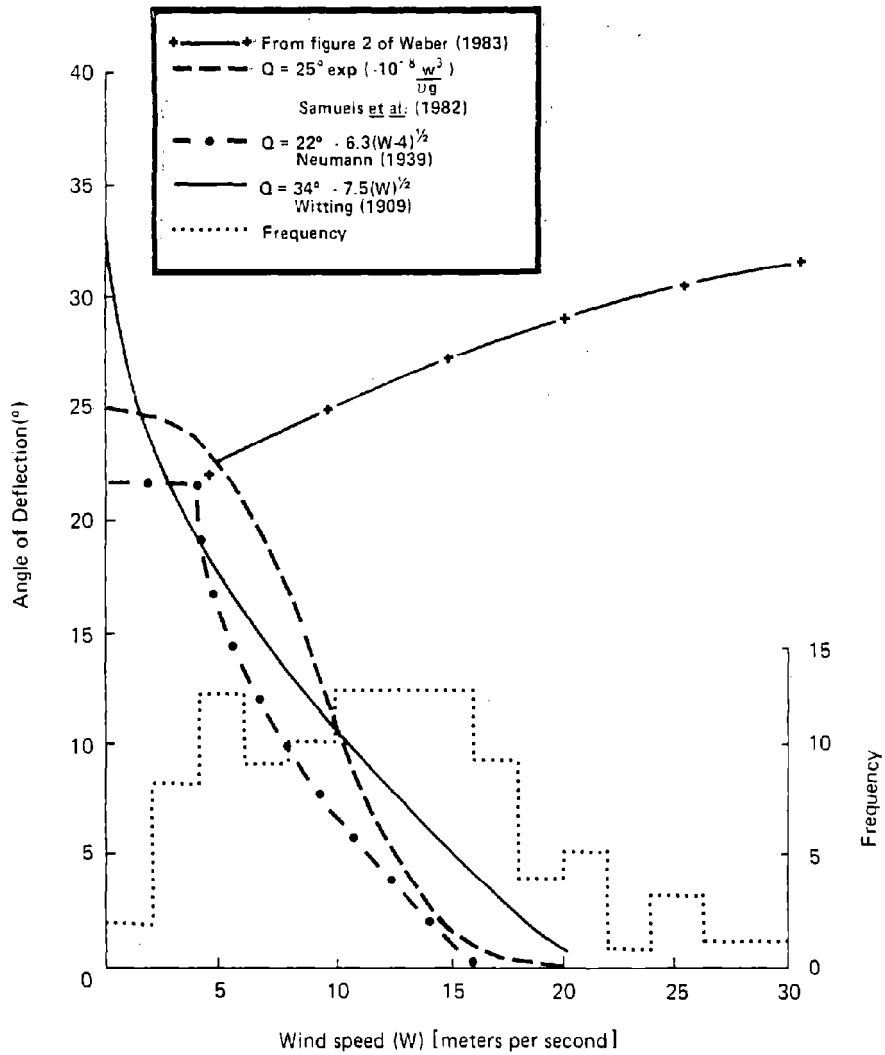


Figure 19.--A comparison of four empirical functions for computing angle of deflection of the surface current to the right of the wind versus wind speed. Average frequency of daily wind speeds (dots) at the three drifter locations by 2 m/sec bins (100 days total).

DAILY PROGRESSIVE VECTORS
FROM 7/17/78
TO 12/31/78

OCEAN CURRENTS
(WIND = 1.0)
(GEOSTROPHIC = 1.0)

BATHYMETRY
200 M ----
2000 M ---

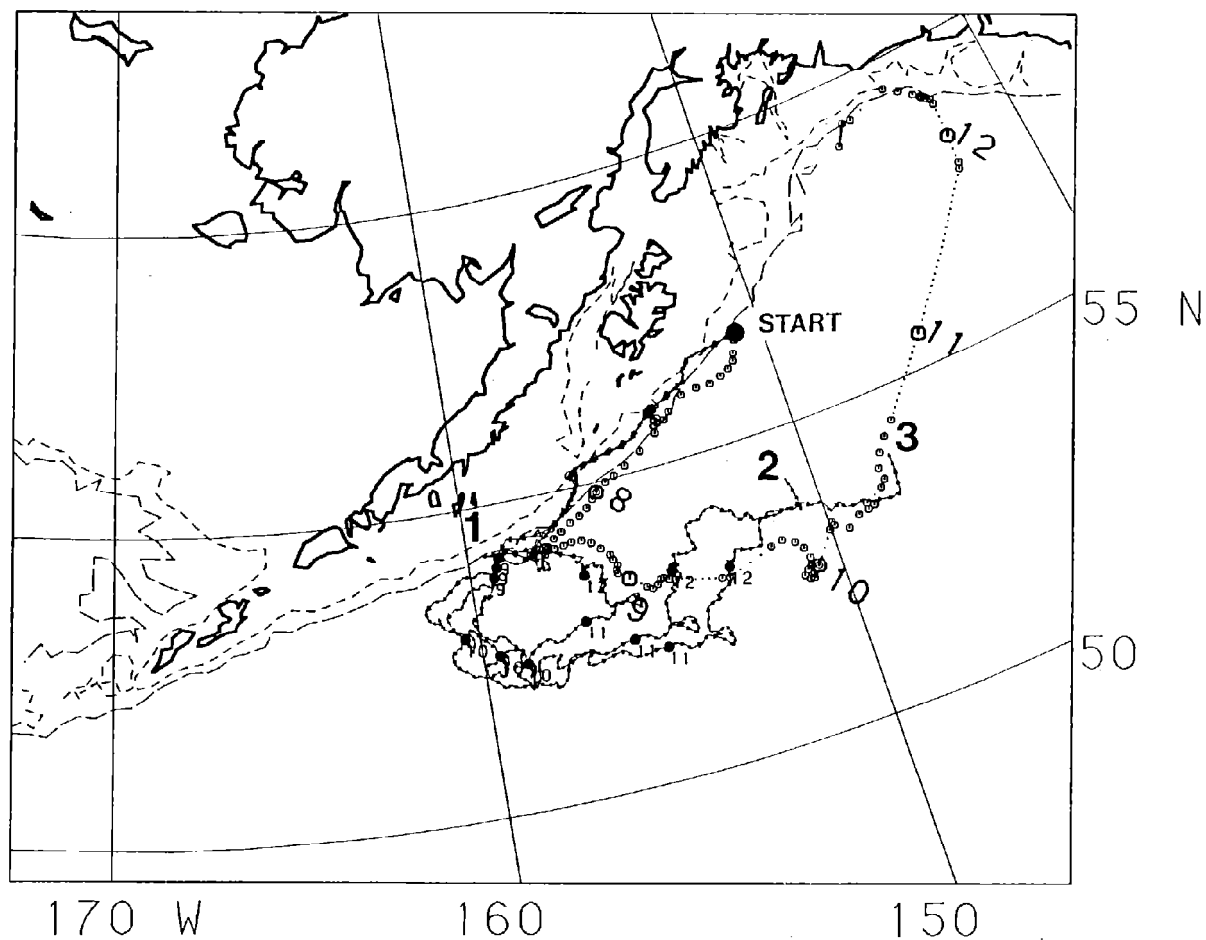


Figure 20. --Three daily progressive vector tracks started on 17 July. Three angles of deflection functions are compared--1) Witting, 2) constant 20 degrees, and 3) constant 30 degrees--for the same speed function (Witting).

the location where drifter No. 400 turned offshore was little affected and the speed was still slow, about 60% of the drifter speed. Farther downstream, the runs that started on 13 August at the corner of the Alaskan Stream recirculation (Fig. 21) showed better agreement and also had a more realistic speed. We were particularly encouraged by the offshore 21 September runs (Fig. 22a), with run No. 2 (20 degrees) showing all the essential features of the drifter track and speeds of about 80% of the drifter speed. The 21 September runs on drifter tracks No. 561 (Fig. 22b) and No. 753 (Fig. 22c) also confirmed this agreement. These three drifters were released at the same location on the same day, but they drifted for two months and had separated considerably at the end of this time. Drifter No. 400 recirculated first on 13 August at long. 158°W and was farthest east (long. 151°W) on 21 September. Drifter No. 561 began its recirculation at the same place as drifter No. 400 (long. 158°W) but recirculated over 2 weeks later on 2 September and ended up between the others at long. 155°W on 21 September. Drifter No. 753 began to recirculate on 3 September but at a location much farther downstream (long. 165°W), and by 21 September had reached only long. 162°W. We concluded from visual inspection that a constant angle of deflection between 20 and 30 degrees gave the best fit, but that speed and angle must be tuned together to take into consideration their mutual interaction.

DAILY PROGRESSIVE VECTORS

FROM 8/13/78

TO 12/31/78

OCEAN CURRENTS

(WIND = 1.0)

(GEOSTROPHIC = 1.0)

BATHYMETRY

200 M - - - -

2000M - - - -

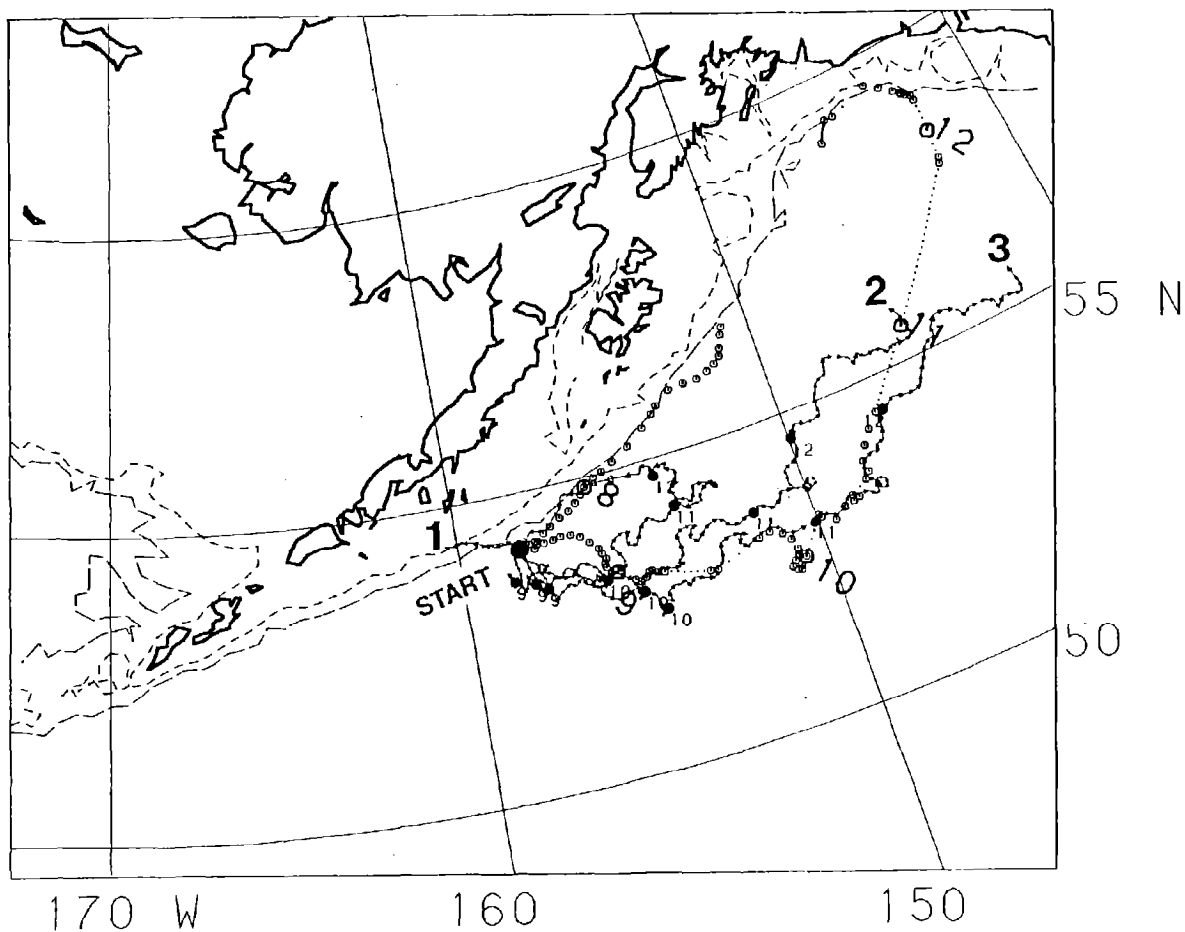


Figure 21. --Three daily progressive vector tracks started at the location of drifter No. 400 on 13 August. The same three angles of deflection functions (Fig. 20) are compared for runs started downstream at the beginning of recirculation.

DAILY PROGRESSIVE VECTORS

FROM 9/21/78
TO 12/31/78

OCEAN CURRENTS

(WIND = 1.0)
(GEOSTROPHIC = 1.0)

BATHYMETRY

200 M ----
2000M - - - -

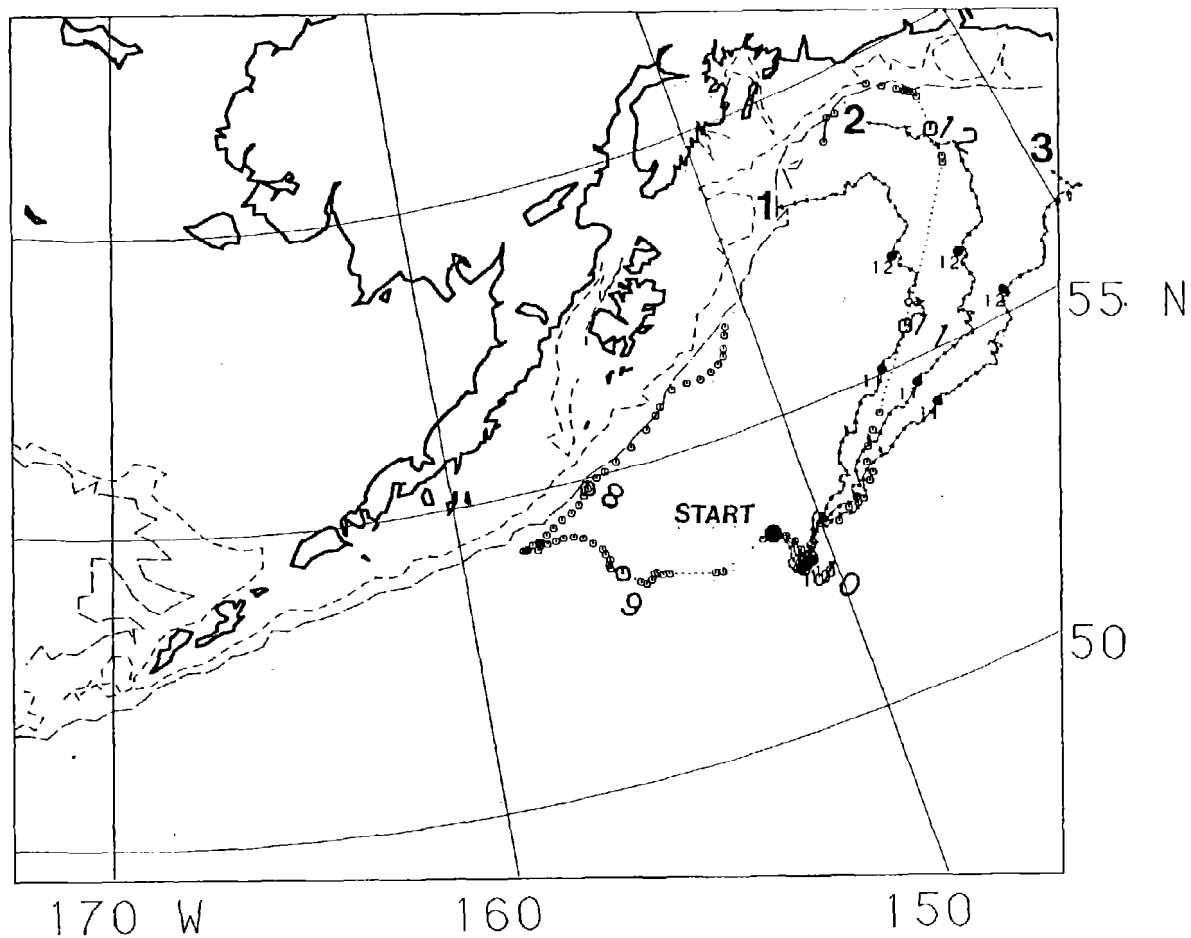


Figure 22(a). --Three daily progressive vector tracks started at the location of drifter No. 400 on 21 September. Three angle of deflection functions are compared--1) Witting, 2) constant 20 degrees, and 3) constant 30 degrees--for the same speed function (Witting).

DAILY PROGRESSIVE VECTORS

FROM 9/21/78

TO 12/31/78

OCEAN CURRENTS

(WIND = 1.0)

(GEOSTROPHIC = 1.0)

BATHYMETRY

200 M ----

2000M ---

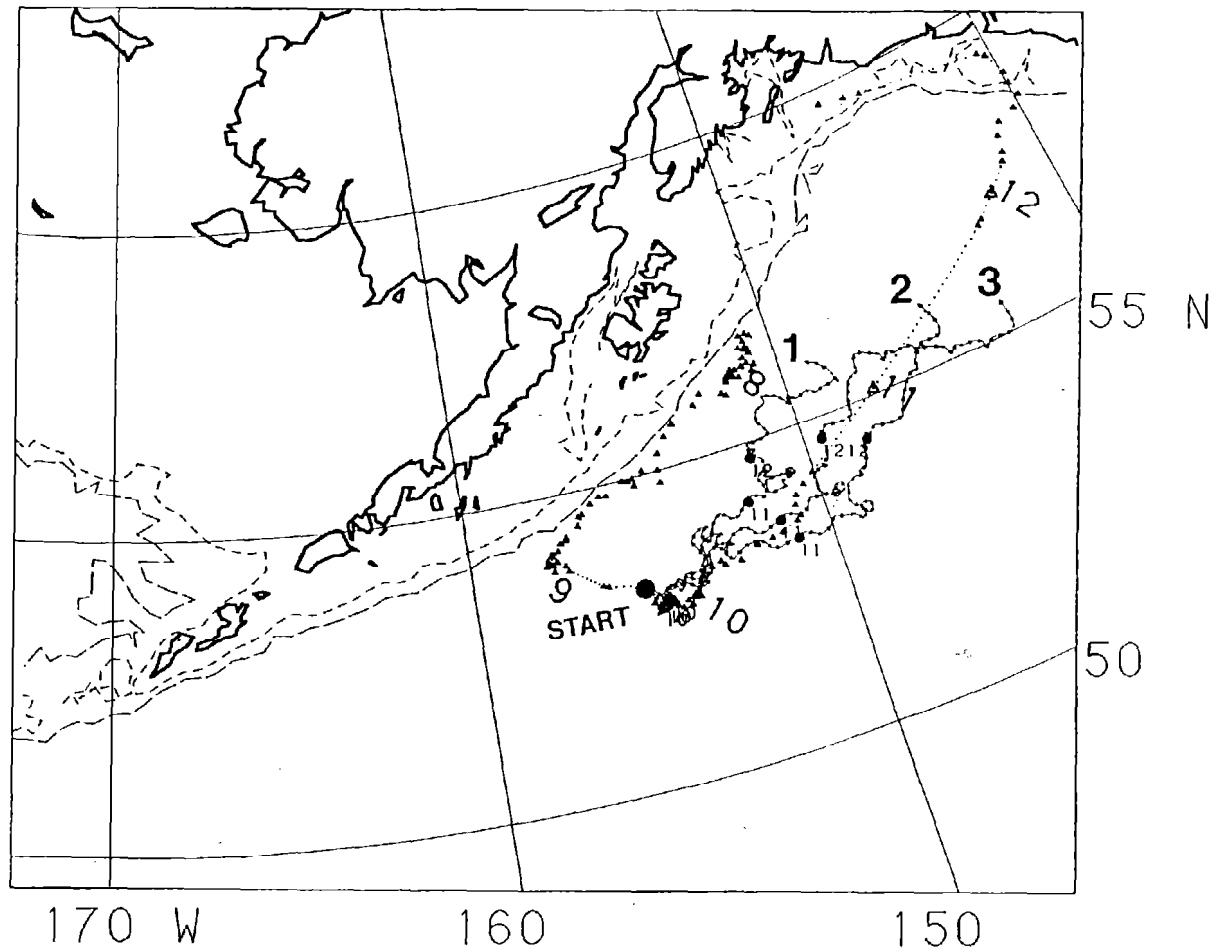


Figure 22(b).--Three daily progressive vector tracks started at the location of drifter No. 561 on 21 September. Three angle of deflection functions are compared--1) Witting, 2) constant 20 degrees, and 3) constant 30 degrees--for the same speed function (Witting).

DAILY PROGRESSIVE VECTORS

FROM 9/21/78

TO 12/31/78

OCEAN CURRENTS

(WIND = 1.0)

(GEOSTROPHIC = 1.0)

BATHYMETRY

200 M - - - -

2000M - - - -

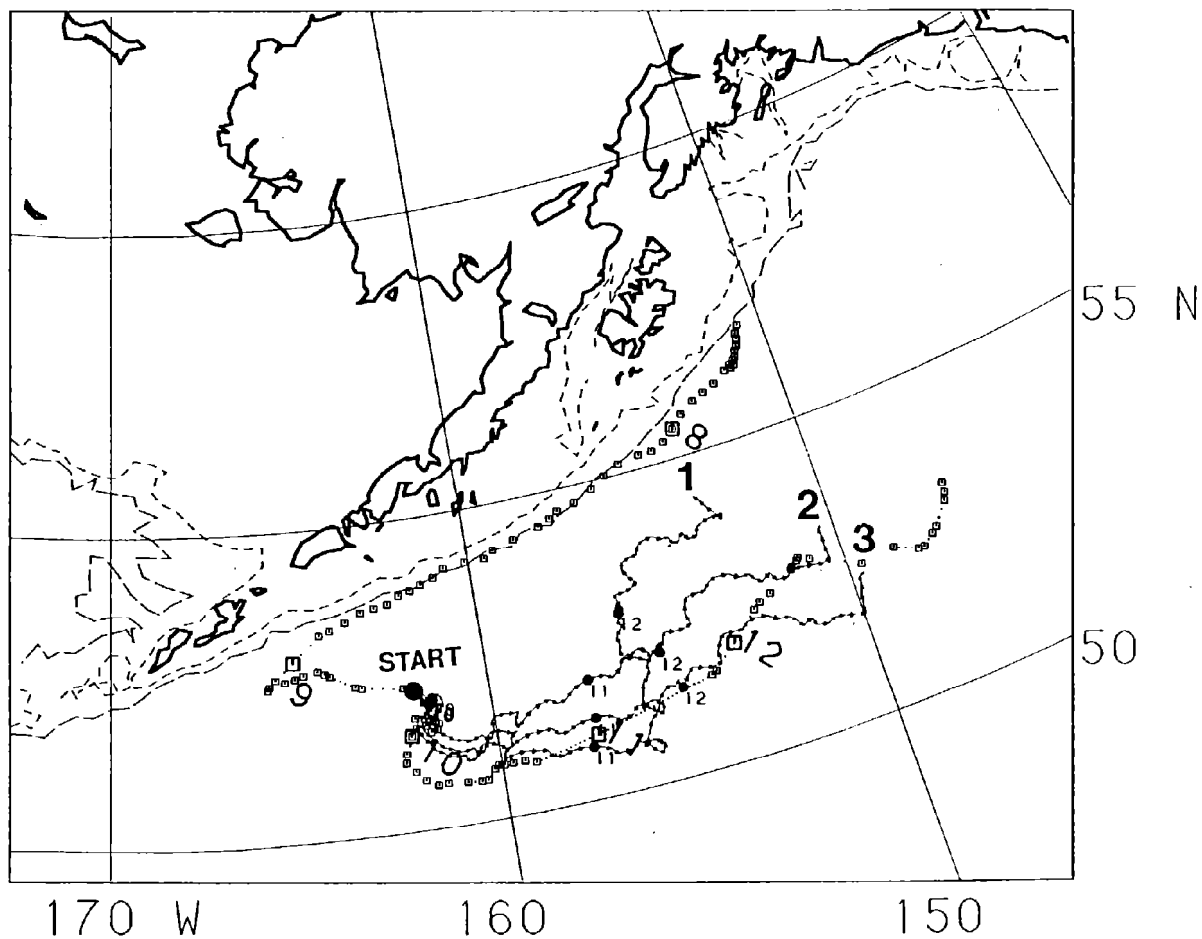


Figure 22(c) .--Three daily progressive vector tracks started at the location of drifter No. 753 on 21 September. Three angle of deflection functions are compared--1) Witting, 2) constant 20 degrees, and 3) constant 30 degrees--for the same speed function (Witting).

Final Tuning Factors

We will examine two time scales in selecting the final tuning factors (wind, geostrophic, and deflection angle) which determine a best-fit model-drifter agreement. The larger scale models an offshore portion of the track between 21 September and 31 December (100 days). The zoom scale models a subset from 21 September to 18 October (26 days), because that portion of the track had the best frequency of satellite readings to verify the daily drifter positions (nearly daily). The wind speed tuning factor is a linear multiplier of the Witting formula, and we use a separate linear tuning factor as a multiplier of the geostrophic component.' In this analysis, we made runs with a combination of tuning factors of 1.0, 1.1, 1.2, 1.3, and 1.4. This allowed us to examine the effect of increasing the wind current or the geostrophic current by increments of 10% while varying the deflection angles from a constant 20 degrees to a constant 30 degrees. Refer to Figure 22 for runs with the baseline or 1.0 wind speed factor.

For drifter No. 400, the best combination of tuning factors was a wind factor of 1.2 and a geostrophic factor of 1.2 (Fig. 23). Run No. 1 with a constant angle of deflection of 20 degrees showed a very close agreement to the drifter track, while the track for a constant 30 degrees turned considerably to the right. Although the 1 December location on the model track (small 12) did not quite reach the drifter's location on 1 December (large 12) (indicating that the speed of the model over the large scale was slightly slower), the match was nearly

DAILY PROGRESSIVE VECTORS
FROM 9/21/78
TO 12/31/78

OCEAN CURRENTS
(WIND = 1.2)
(GEOSTROPHIC = 1.2)

BATHYMETRY
200 M - - - -
2000 M - - - -

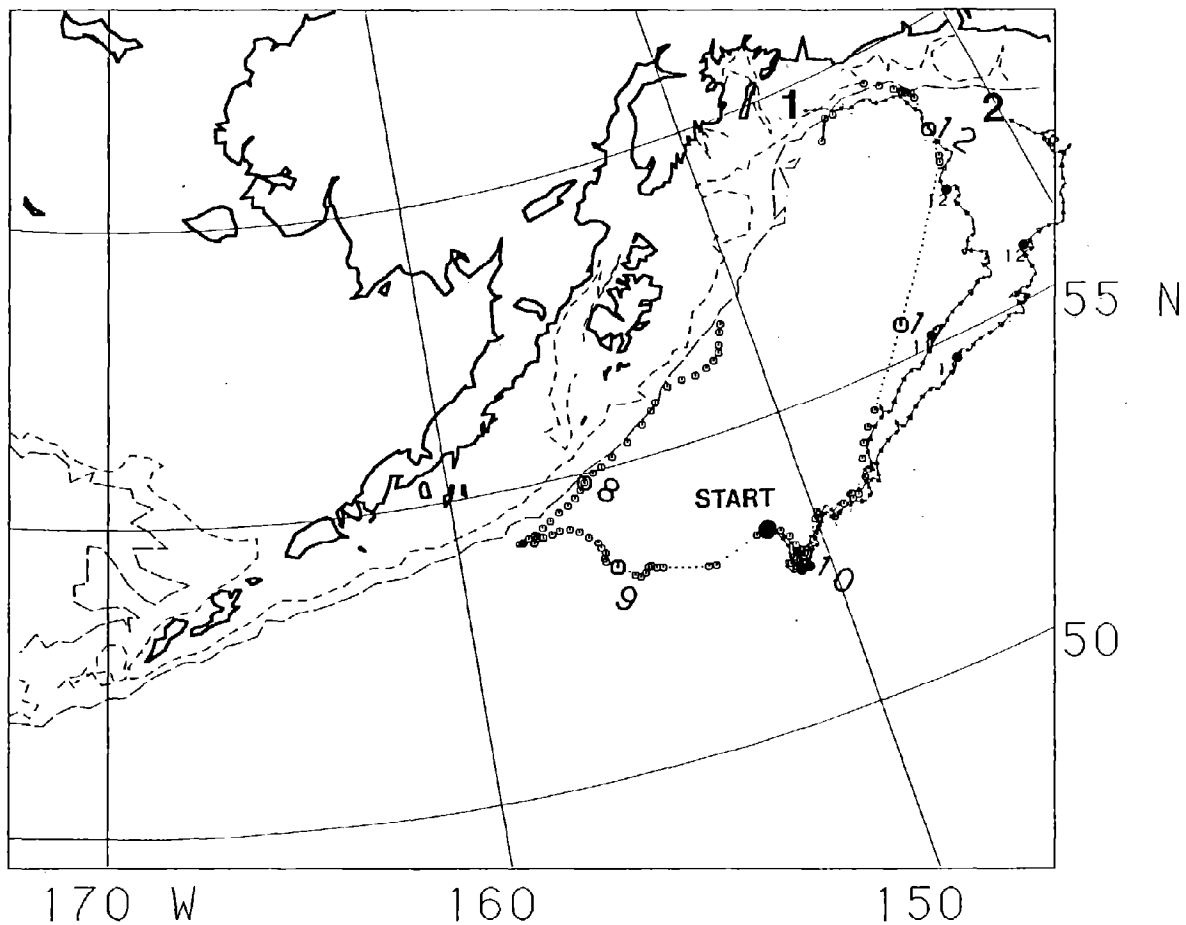


Figure 23.--Drifter No. 400 and daily progressive vector tracks (start = 21 September, end = 31 December, wind = 1.2, geostrophic = 1.2); comparisons for angle of deflection values of 1) 20 degrees and 2) 30 degrees. Model track No. 2 shows best fit.

perfect over the zoom scale (Fig. 24). We have presented tracks using the three angle of deflection functions on the small scale with wind = 1.0, 1.2, and 1.4 (Figs. 25(a), 25(b), and 25(c), respectively) to show a convincing perspective that the constant 20 degree angle (run No. 2, Fig. 25b) is the best choice for closest fit to drifter track No. 400. Because the same overall speed increase from tuning (wind = 1.2, geostrophic = 1.2) may also be obtained by decreasing the wind factor to 1.0 and increasing the geostrophic factor to 1.5, we made five runs increasing the geostrophic factor by increments of 0.1. One representative track (wind = 1.0, geostrophic = 1.5, deflection angle = 20 degrees) showed the similarity (Fig. 26), but it was not better than the previously chosen best-fit track (wind = 1.2, geostrophic = 1.2, deflection angle = 20 degrees), especially considering the resolution of the model which is estimated by the visual scatter of several other model tracks started two days apart over this same zoom portion of the drifter track (Fig. 27).

The results for drifter No. 561 were suspect. Much of the satellite position data was questionable when compared to tracks of the other two drifters. Computed tracks (start = 21 September, wind = 1.2, geostrophic = 1.2, deflection angle = 20 degrees) slightly west of drifter No. 400's location on the same date for each of the three angle functions (Fig. 28) showed a similar angular relationship to drifter track No. 561 but much slower speeds. Trial runs indicated that a wind factor of 2.0 would be required to bring the model into approximate agreement with the drifter. 'This unacceptably large factor confirmed that

DAILY PROGRESSIVE VECTOR DISTANCE
FROM 78 - 9 - 21
TO 78 - 10 - 18

SURFACE OCEAN CURRENTS
(WIND = 1.20)
(GEOSTROPHIC = 1.20)

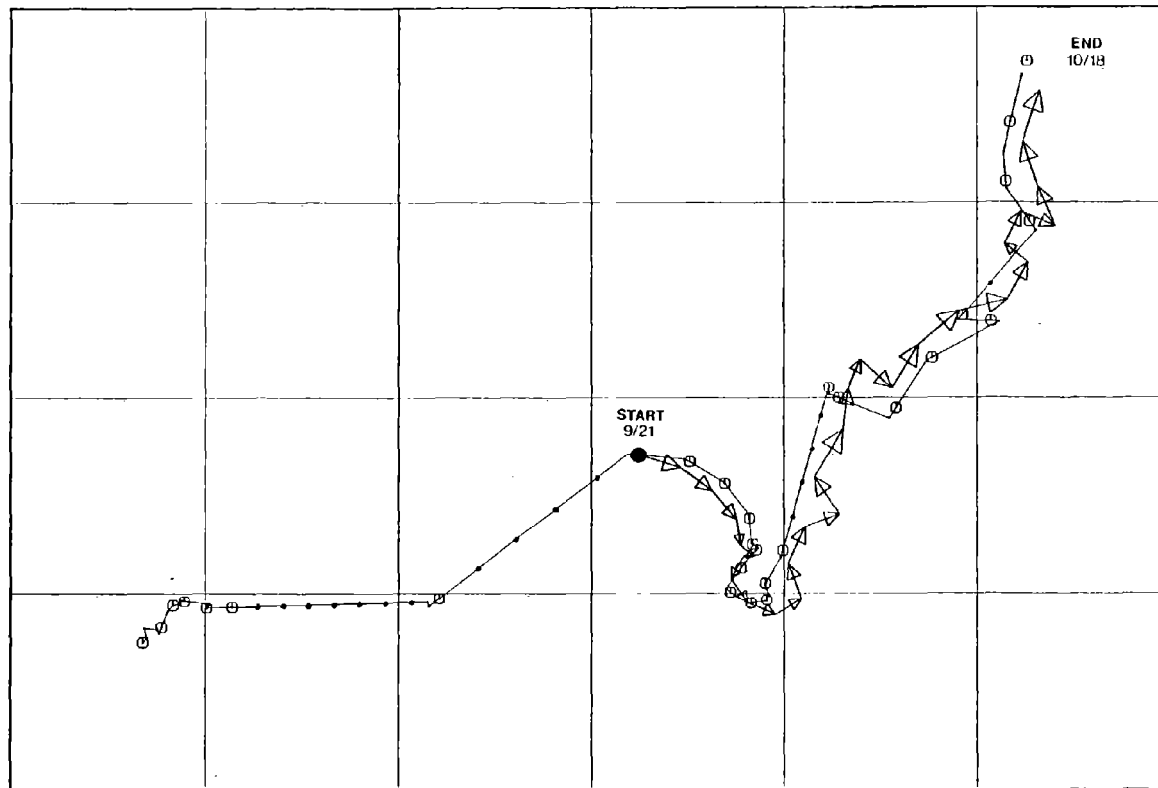


Figure 24. --Drifter No. 400 and daily progressive vector tracks (start = 21 September, end = 18 October, wind = 1.2, geostrophic = 1.2, deflection angle = 20 degrees); zoom scale plot of best fit model run.

DAILY PROGRESSIVE VECTOR DISTANCE
FROM 78 - 9 - 21
TO 78 - 10 - 18

SURFACE OCEAN CURRENTS
(WIND = 1.00)
(GEOSTROPHIC = 1.20)

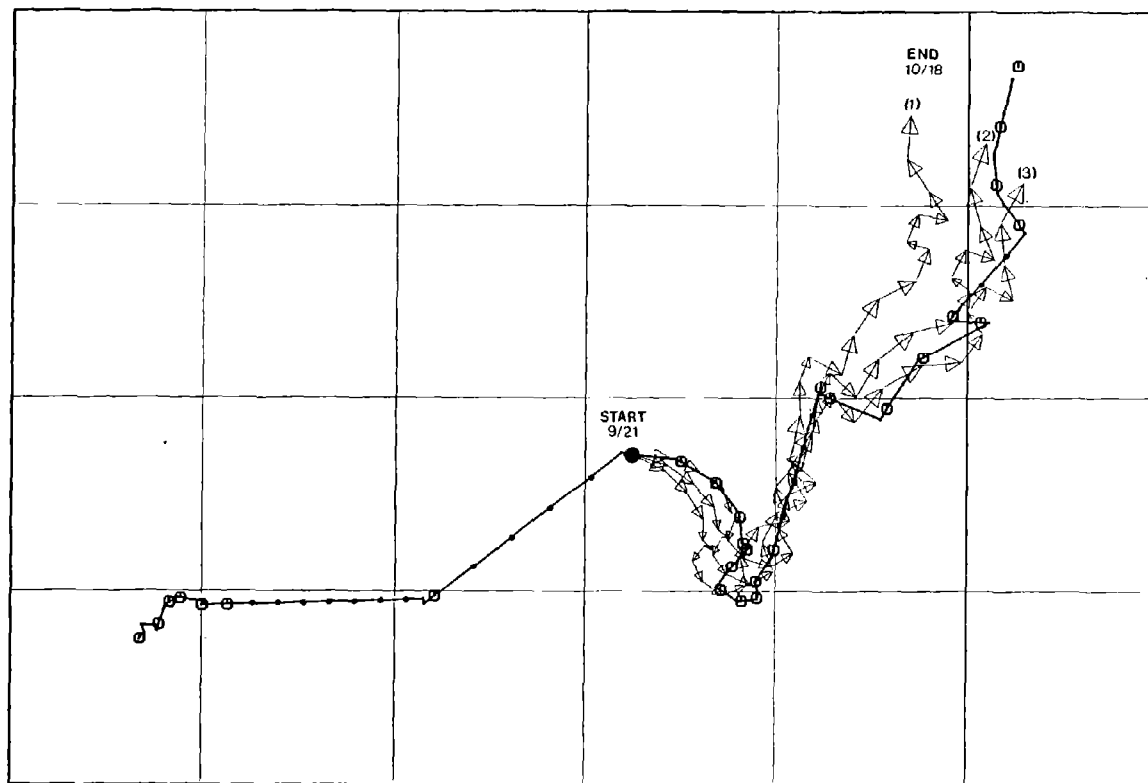


Figure 25(a).--Drifter No. 400 and daily progressive vector tracks (start = 21 September, end = 18 October, wind = 1.0, geostrophic = 1.2); comparison of three angle of deflection functions; 1) Witting, 2) 20 degrees, and 3) 30 degrees. First in a series wind = 1.0, 1.2, and 1.4.

DAILY PROGRESSIVE VECTOR DISTANCE

FROM 78 - 9 - 21
TO 78 - 10 - 18

SURFACE OCEAN CURRENTS

(WIND = 1.20)
(GEOSTROPHIC = 1.20)

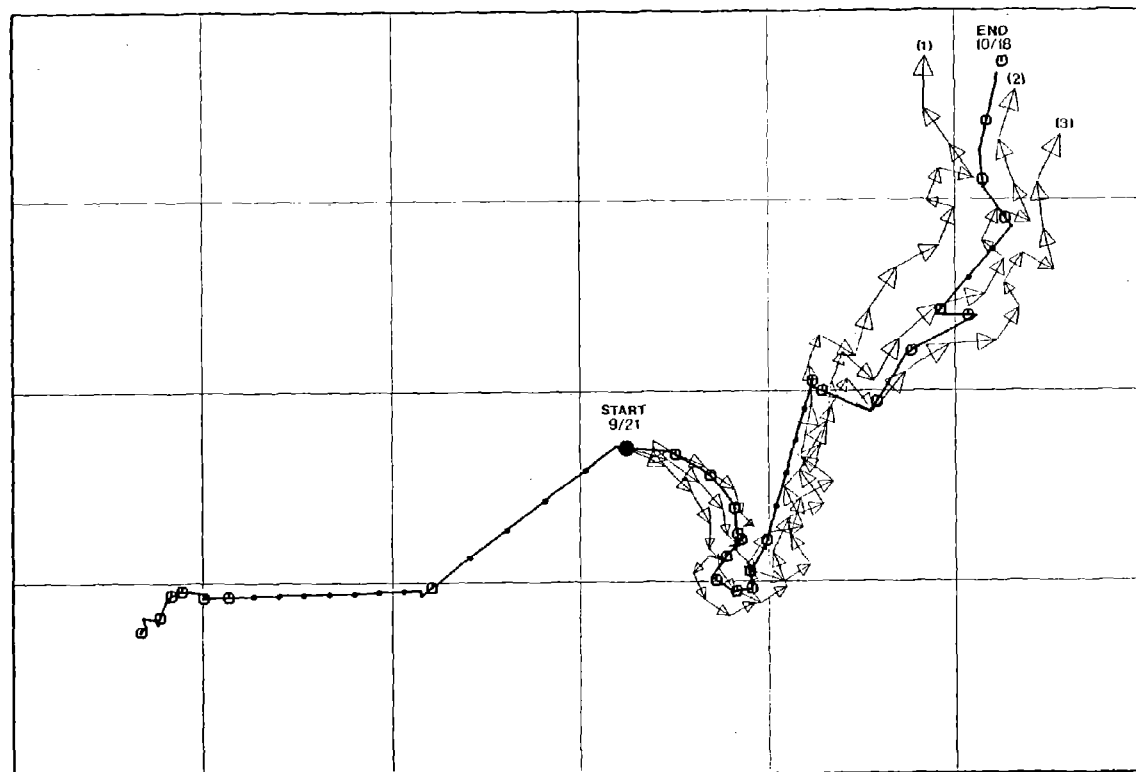


Figure 25(b).--Drifter No. 400 and daily progressive vector tracks (start = 21 September, end = 18 October, wind = 1.2, geostrophic = 1.2); comparison of three angle of deflection functions: 1) Witting, 2) 20 degrees, and 3) 30 degrees. Second in a series, wind = 1.0, 1.2, and 1.4.

DAILY PROGRESSIVE VECTOR DISTANCE

FROM 78 - 9 - 21

TO 78 - 10 - 18

SURFACE OCEAN CURRENTS

(WIND = 1.40)

(GEOSTROPHIC = 1.20)

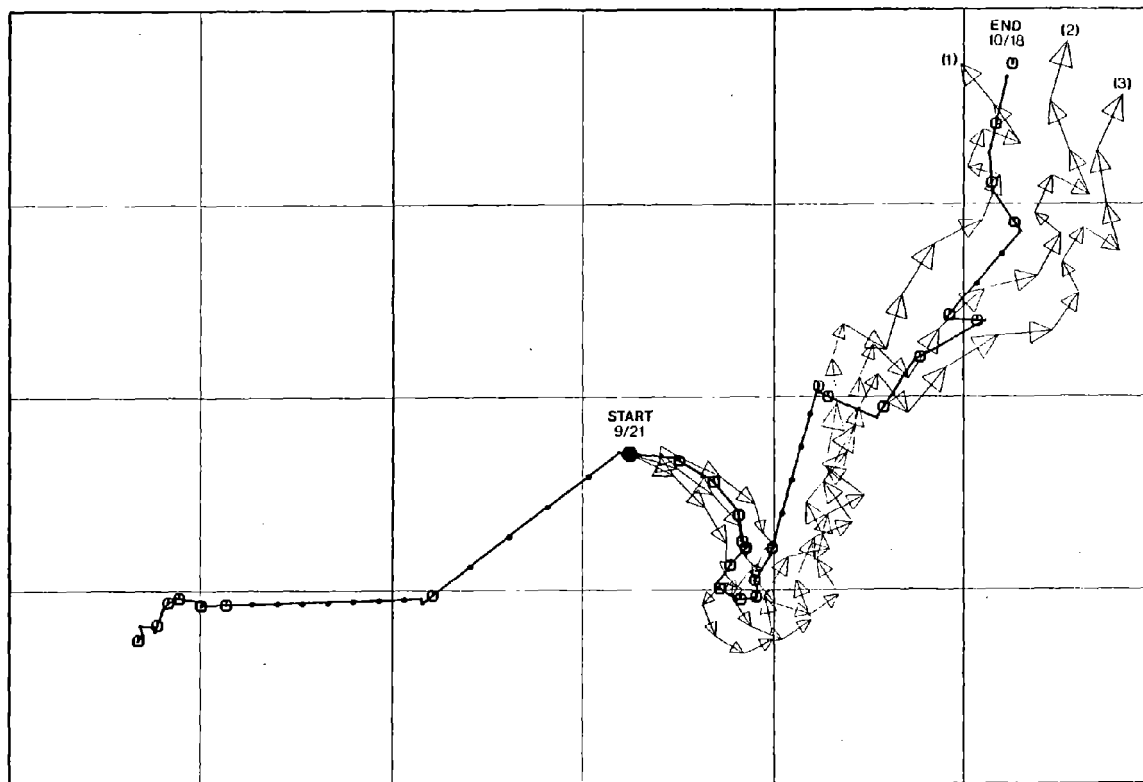


Figure 25(c).--Drifter No. 400 and daily progressive vector tracks (start = 21 September, end = 18 October, wind = 1.4, geostrophic = 1.2); comparison of three angle of deflection functions: 1) Witting, 2) 20 degrees, and 3) 30 degrees. Third in a series, wind = 1.0, 1.2, and 1.4.

DAILY PROGRESSIVE VECTORS

FROM 9/21/78
TO 12/31/78

OCEAN CURRENTS

(WIND = 1.2)
(GEOSTROPHIC = 1.2)

BATHYMETRY

200 M ----
2000 M ---

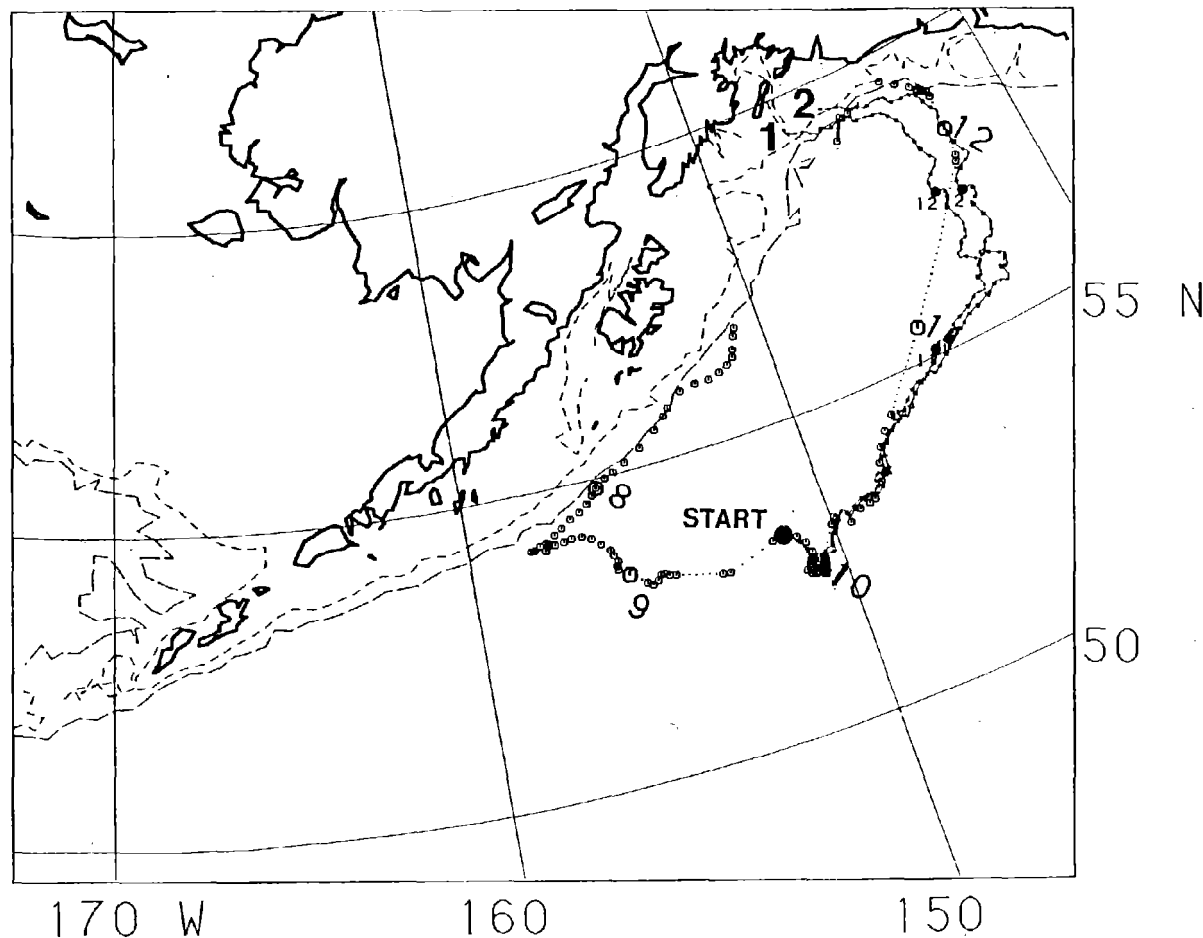


Figure 26. --Drifter No. 400 and daily progressive vector tracks. Run No. 1 (start = 21 September, end = 31 December, wind = 1.0, geostrophic = 1.5, angle = 20 degrees) compared with run No. 2 (start = 21 September, end = 31 December, wind = 1.2, geostrophic = 1.2, angle = 20 degrees). This shows that an increase in geostrophic speed only is not sufficient.

DAILY PROGRESSIVE VECTORS
FROM 10/10/78
TO 12/31/78

OCEAN CURRENTS
(WIND = 1.2)
(GEOSTROPHIC = 1.2)

BATHYMETRY
200 M - - - -
2000M - - - -

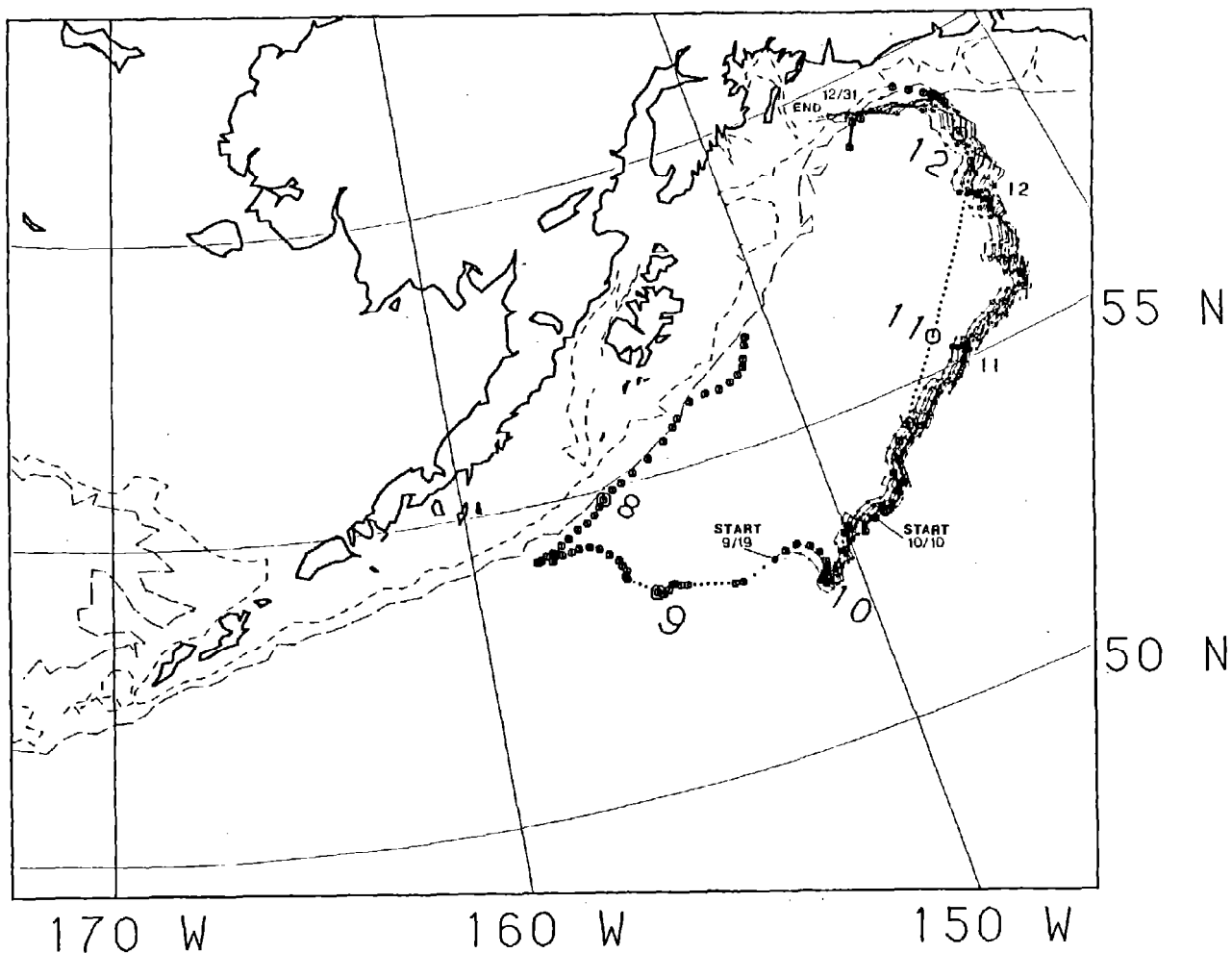
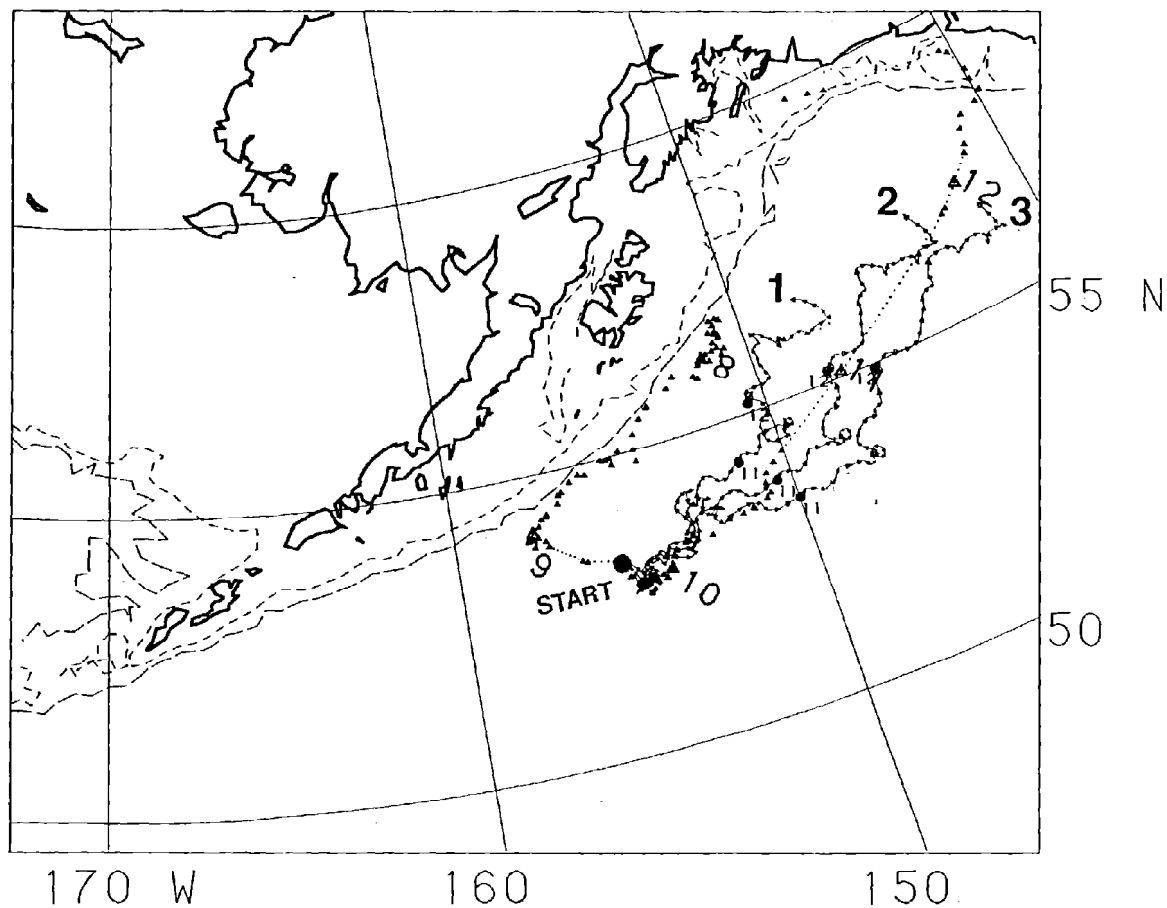


Figure 27. --Drifter No. 400 and a composite plot of eleven daily progressive vector tracks from model runs with the same best fit tuning factors but started at the 0000Z drifter locations 2 days apart on 19, 21, 23, 25, 27, and 29 September, also 2, 4, 6, 8, and 10 October.

DAILY PROGRESSIVE VECTORS
FROM 9/21/78
TO 12/31/78

OCEAN CURRENTS
(WIND = 1.2)
(GEOSTROPHIC = 1.2)

BATHYMETRY
200 M ----
2000 M ---



55

Figure 28. --Drifter No. 561 and daily progressive vector tracks (start = 21 September, end = 31 December, wind = 1.2, geostrophic = 1.2); comparisons for angle of deflection functions: 1) Witting, 2) 20 degrees, and 3) 30 degrees. Note much greater speed of this drifter than drifter No. 400 (Fig. 23).

the drifter position data were suspect and precluded further analysis. Fortunately, comparisons of model runs that started along the track of the last drifter (No. 753) confirmed our findings with drifter No. 400, giving credence to our results.

As we did with the other two drifter tracks (Fig. 23 and Fig. 28), we compared the model runs for the three angle of deflection functions to drifter track No. 753 (Fig. 29). On the large scale there is nearly a perfect match over the last month of drift and at the end point. However, this agreement was for an angle of 30 degrees, whereas the angle of drifter No. 400 was 20 degrees. This would seem to lower expectations of accuracy for the model to a 10 degree range (plus or minus 5 degrees), and this was apparently confirmed by the scatter in the composite plot of 11 model tracks (Fig. 30) started 2 days apart between 21 September and 10 October. This scatter or variability seemed excessive, however, and further examination gave more insight into the model's behavior under changing atmospheric conditions. When strong storms pass by slowly over several days, they cause looping (drifter No. 753) or meandering (drifter No. 400) in the trajectories of objects drifting near the ocean surface. From 23 to 28 September, drifter No. 753 completed such a closed loop, and the model-computed track also followed a closed loop. An enlargement of Figure 30 allowed us to narrow down some of the scatter related to processes which caused the curvature of the drifter's path. The curvature of the drifter track was anticyclonic before the closed cyclonic eddy appeared, and the anticyclonic drift tended to resume for a short while after the

DAILY PROGRESSIVE VECTORS	OCEAN CURRENTS	BATHYMETRY
FROM 9/21/78	(WIND = 1.2)	200 M - - - -
TO 12/31/78	(GEOSTROPHIC = 1.2)	2000 M - - - -

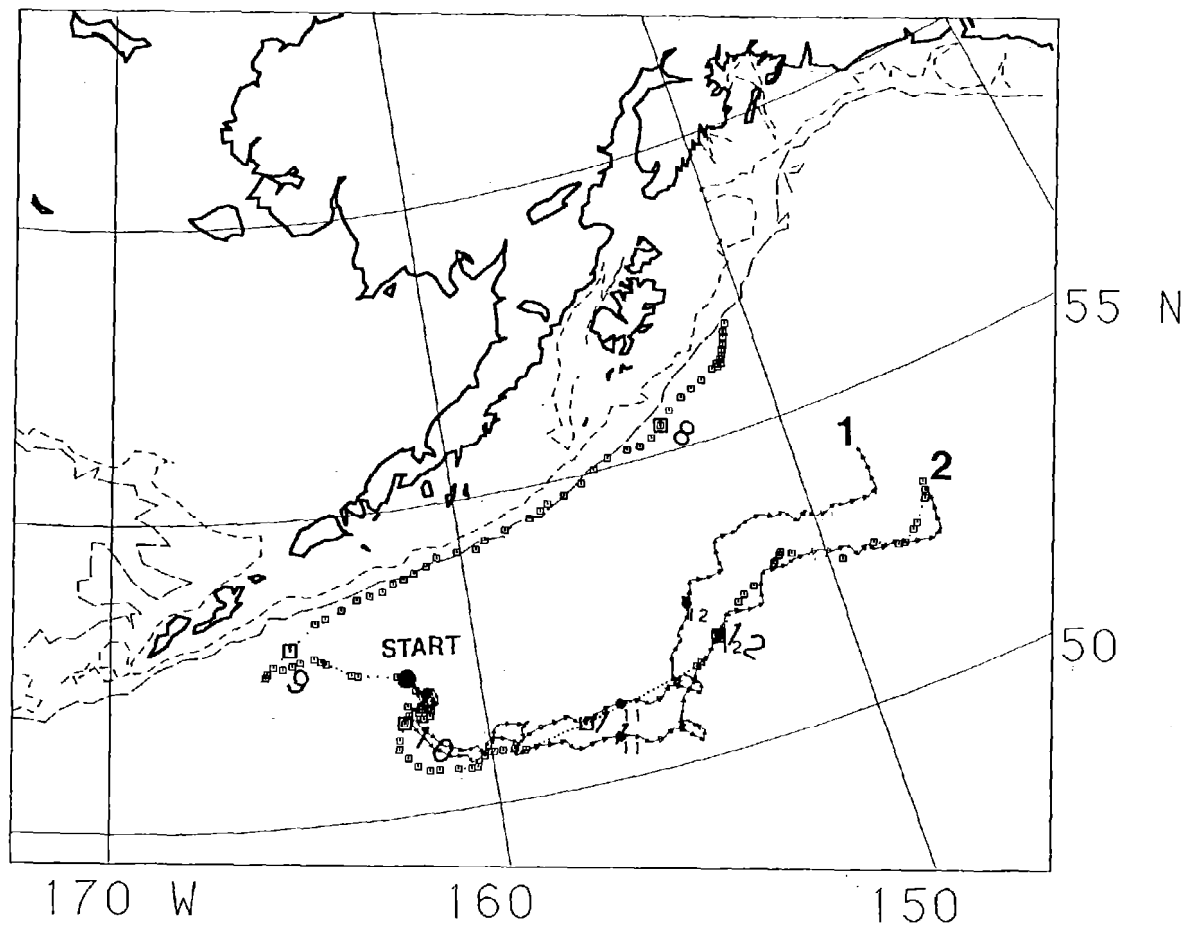


Figure 29.--Drifter No. 753 and daily progressive vector tracks (start = 21 September, end = 31 December, wind = 1.2, geostrophic = 1.2); comparison for deflection angles of 1) 20 degrees and 2) 30 degrees. Best fit appears to be run No. 2.

DAILY PROGRESSIVE VECTORS
FROM 10/10/78
TO 12/31/78

OCEAN CURRENTS
(WIND = 1.2)
(GEOSTROPHIC = 1.2)

BATHYMETRY
200 M - - - -
2000 M - - - -

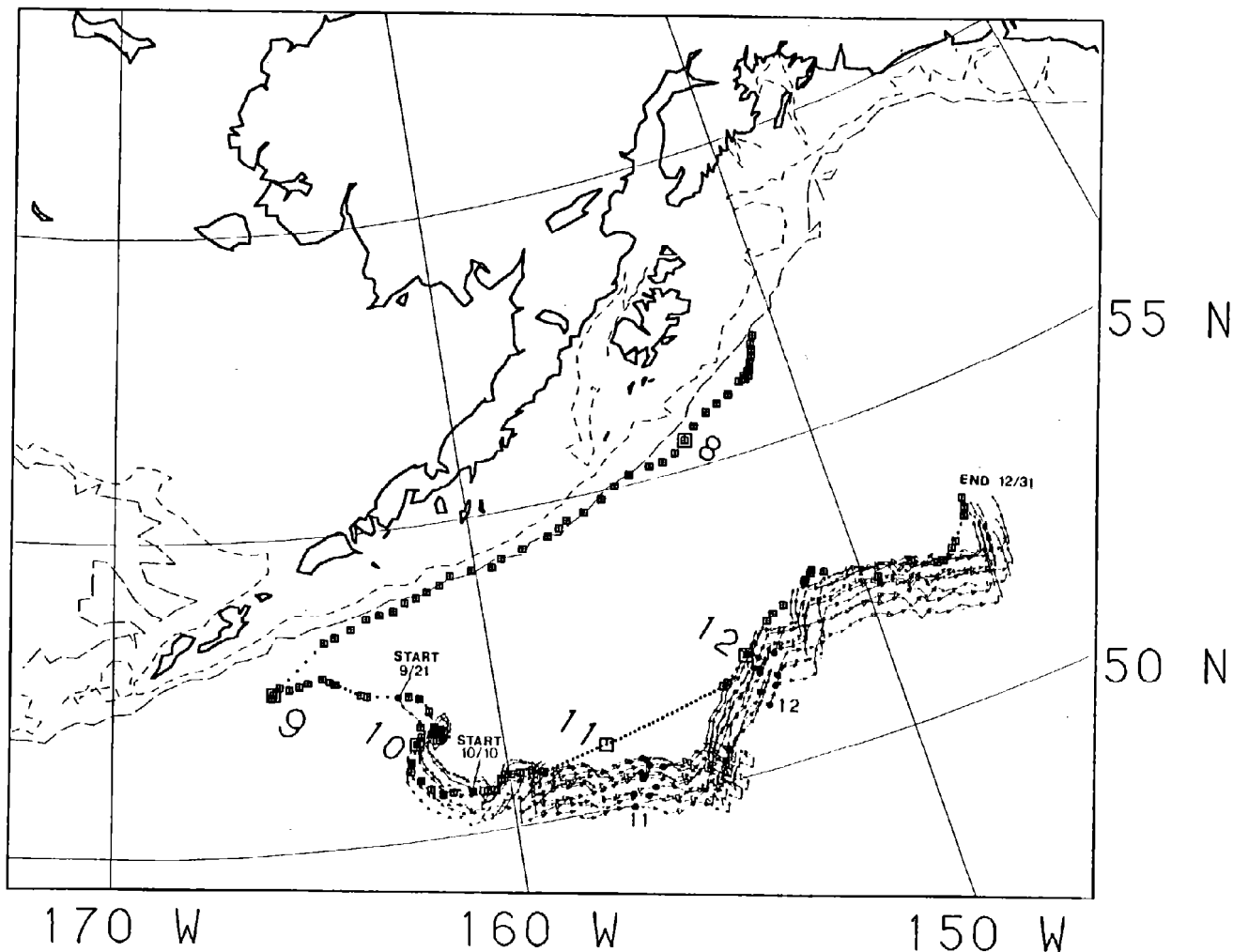


Figure 30.--Drifter No. 753 and a composite plot of eleven daily progressive vector tracks from model runs with the same tuning factors but started at the 0000Z drifter locations 2 days on 19 21 23, 25, 27, and 29 September, also 2, 4, 6, 8, apart and 10 October. Note larger scatter than in Figure 27

eddy. All model tracks that began before 1 October tended to stay to the left of the drifter track (Fig. 31(a)), while all the model tracks started after 1 October, when the curvature of the track reversed to cyclonic, tended to stay to the right of the drifter track (Fig. 31(b)). Although this is yet to be explained, it points out that the straighter portions of the track would provide better locations from which to start model runs. Places where the inflection in curvature changes sign, such as on 29 September, provide similar representative start locations. Replotting Figure 29 for a 29 September starting point (Fig. 32) gave us a more accurate assessment of the best-fit angle of deflection midway between 20 and 30 degrees. We can find no significantly better match than the Weber (1983) function (Fig. 33(a) and Fig. 33(b) --zoom) for the appropriate angle of deflection.

Now that we have established the 1.2 multiplication factor for current speed computation functions (wind and geostrophic) and Weber's function for the angle of deflection (averages about 26 degrees), this tuning phase for OSCURS is completed. Subsequent publications will discuss applications of the model to investigations of interannual variability of ocean currents.

DAILY PROGRESSIVE VECTOR DISTANCE
FROM 9/23/78
TO 10/19/78

SURFACE OCEAN CURRENTS
(WIND + GEOSTROPHIC COMPONENT)
(X1.20. X 1.20)

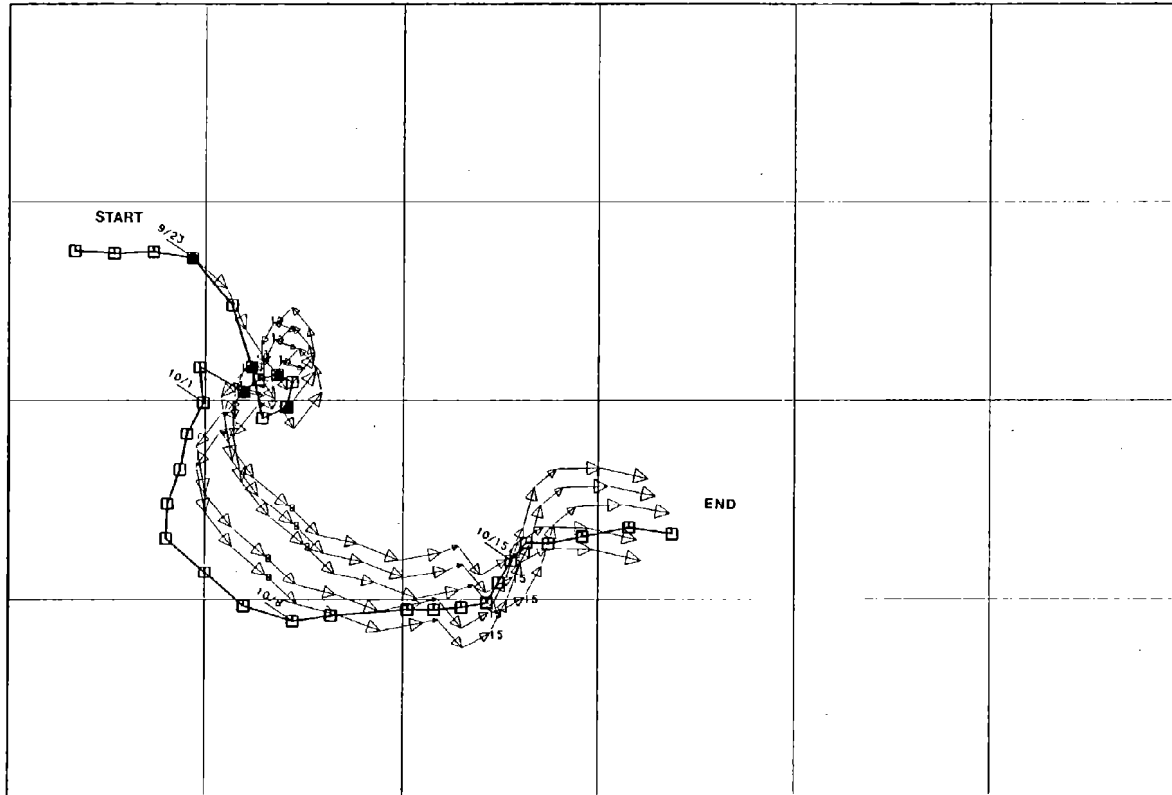


Figure 31(a).--Drifter No. 753 and a composite plot of five daily progressive vector tracks from model runs- with the same tuning factors (wind = 1.2, geostrophic = 1.2, deflection angle = 30 degrees) but started at 0000Z drifter locations 2 days apart on 21, 23, 25, 27, and 29 September, Note that model tracks tend to stay to the left of the drifter track.

DAILY PROGRESSIVE VECTOR DISTANCE
FROM 10/02/78
TO 10/19/78

SURFACE OCEAN CURRENTS
(WIND + GEOSTROPHIC COMPONENT)
(X1.20, X 1.20)

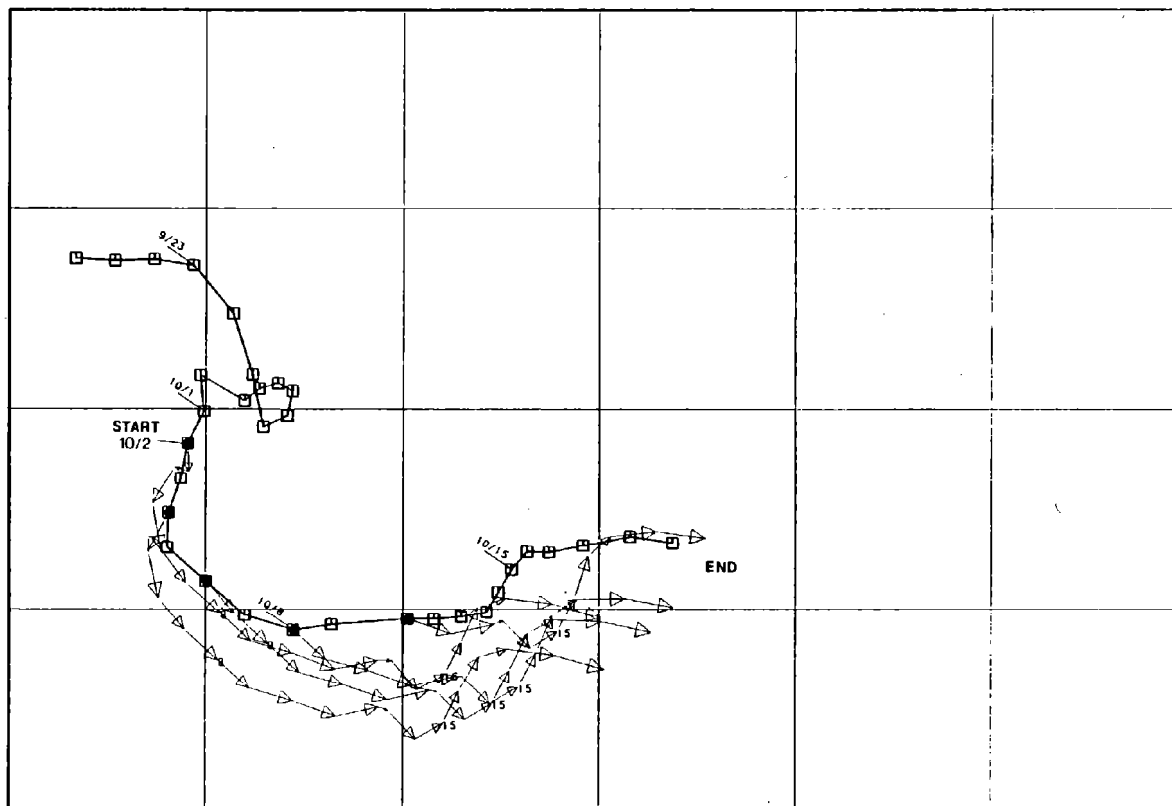


Figure 31(b).--Drifter No. 753 and a composite plot of five daily progressive vector tracks from model runs with the same tuning factors (wind = 1.2, geostrophic = 1.2, deflection angle = 30 degrees) but started at 0000Z drifter locations 2 days apart on 2, 4, 6, 8, and 10 October. Note that model tracks tend to stay to the right of the drifter track, contrary to Figure 31(a).

DAILY PROGRESSIVE VECTORS

FROM 9/29/78

TO 12/31/78

OCEAN CURRENTS

(WIND = 1.2)

(GEOSTROPHIC = 1.2)

BATHYMETRY

200 M ----

2000M ---

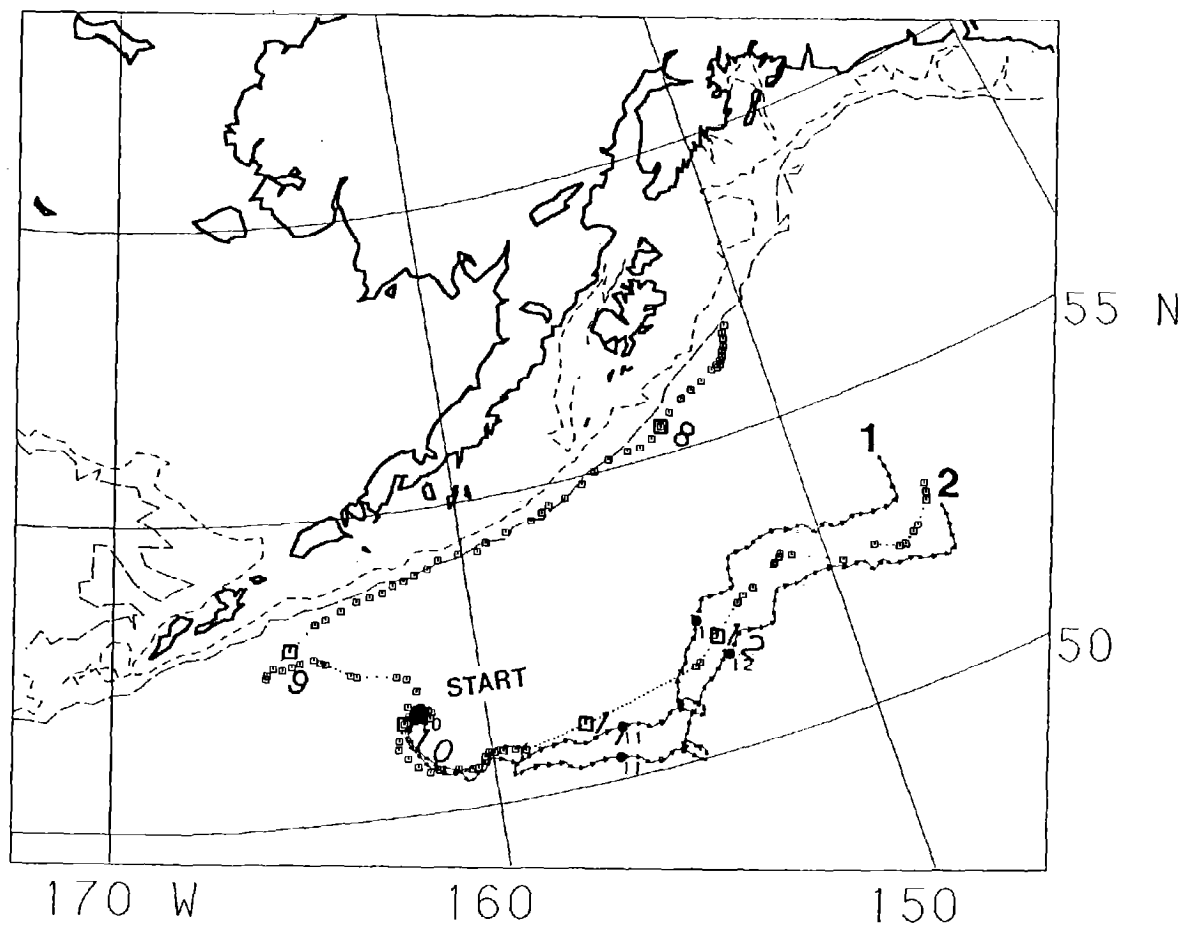


Figure 32.--Drifter No. 753 and daily progressive vector tracks (start = 29 September, end = 31 December, wind = 1.2, geostrophic = 1.2); comparison for deflection angles of 1) 20 degrees and 2) 30 degrees. Best fit appears to be about 26 degrees.

DAILY PROGRESSIVE VECTORS

FROM 9/29/78

TO 12/31/78

OCEAN CURRENTS

(WIND = 1.2)

(GEOSTROPHIC = 1.2)

BATHYMETRY

200 M ----

2000M ---

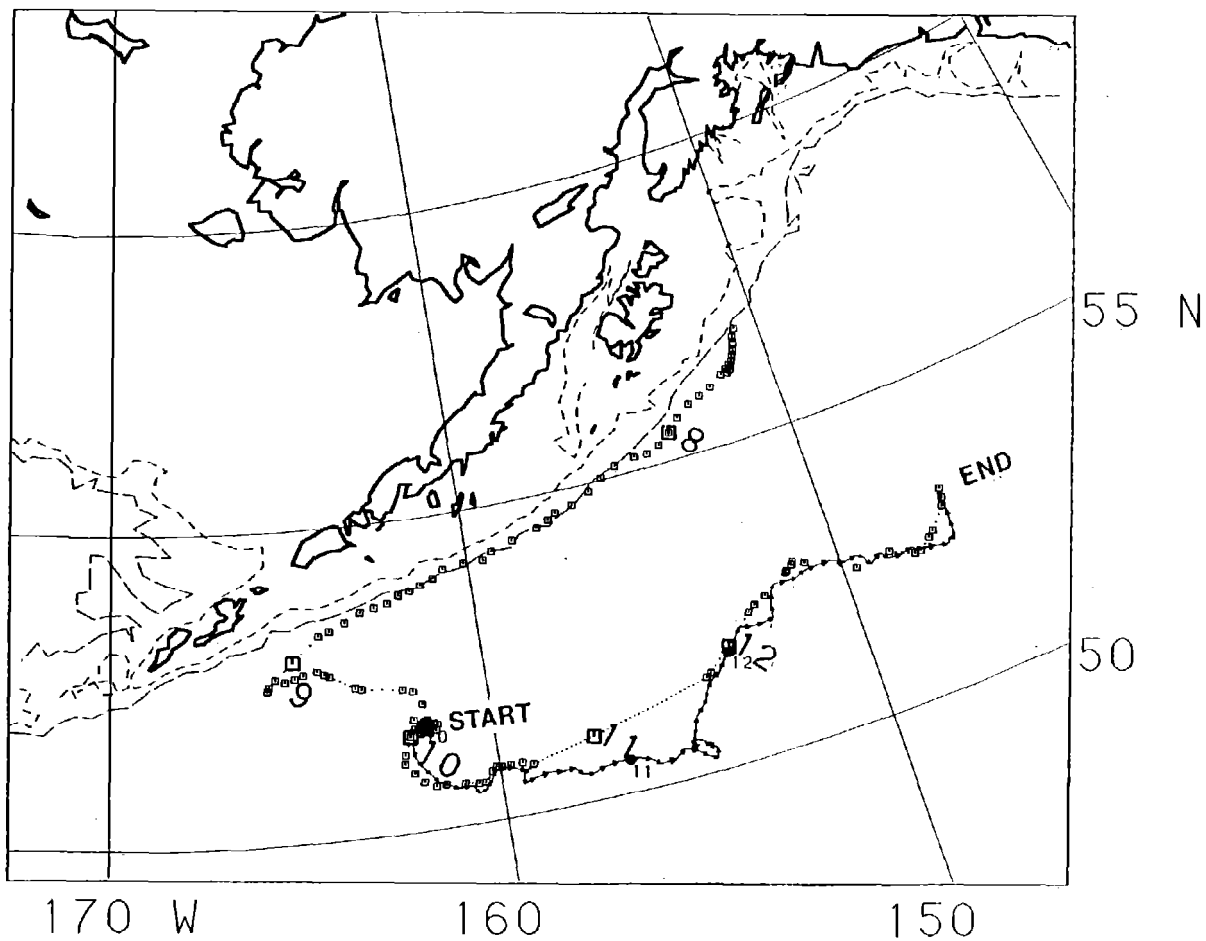


Figure 33(a).--Drifter No. 753 compared to a computed daily progressive vector track (start = 29 September, end = 31 December, wind = 1.2, geostrophic = 1.2, deflection angle = Weber's function). Note exceptional agreement.

DAILY PROGRESSIVE VECTOR DISTANCE
FROM 9/29/78
TO 10/19/78

SURFACE OCEAN CURRENTS
(WIND + GEOSTROPHIC COMPONENT)
(X1.20. X 1.20)

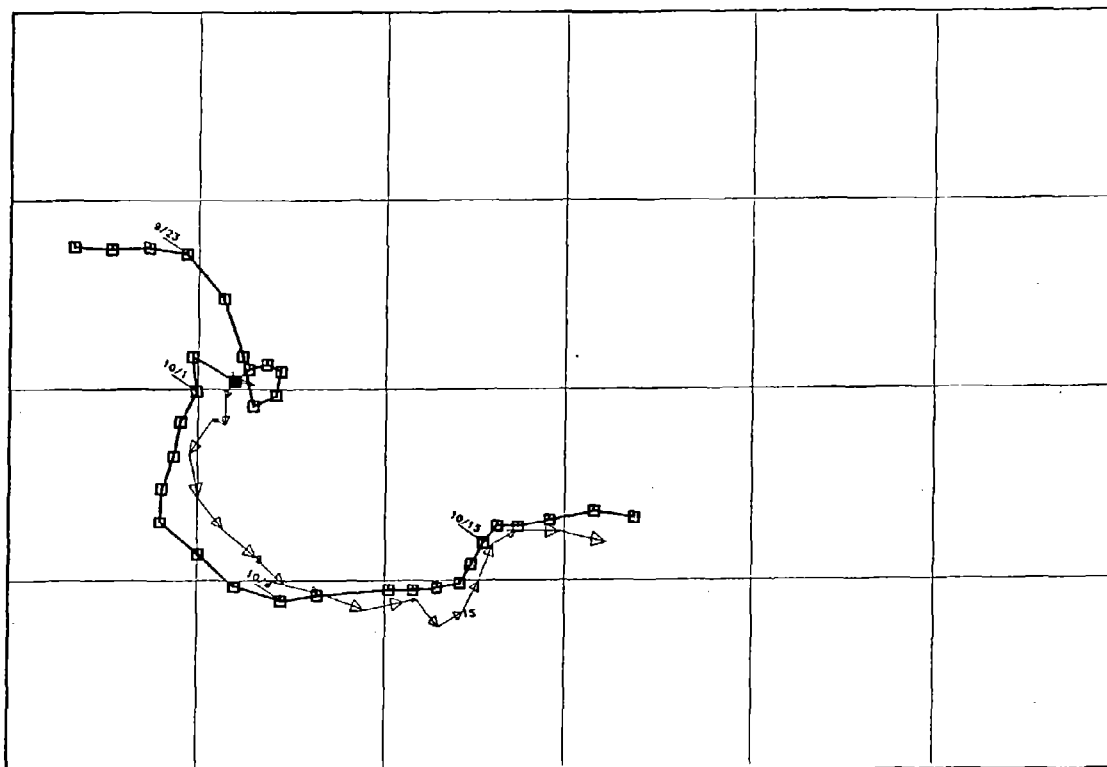


Figure 33(b).--Drifter No. 753 compared to a computed daily progressive vector track (start = 29 December, end = 20 October, wind = 1.2, geostrophic = 1.2, deflection angle = Weber's function). Zoom plot of figure 33(a), shows expanded view of exceptional agreement.

REFERENCES

- Amstutz, D. E., and W. B. Samuels. 1984. Comment on "Steady wind- and wave-induced currents in the open ocean." *J. Phys. Oceanogr.* 14:484-485.
- Bauer, R., and M. Robinson. 1985. Description of the Bauer-Robinson numerical atlas, version VIII, February 1985. Compass Systems, Inc., 4640 Jewell St., #204, San Diego, CA 92109, 13 p.
- Emery, William J., and Kevin Hamilton. 1985. Atmospheric forcing of interannual variability in the Northeast Pacific Ocean: connections with El Nino. *J. Geophys. Res.* 90(C1):857-868.
- Emery, W. J., T. C. Royer, and R. W. Reynolds. 1985. The anomalous tracks of North Pacific drifting buoys 1981 to 1983. *Deep-Sea Res.* 32(3):315-347.
- Favorite, F., A. J. Dodimead, and K. Nasu. 1976. Oceanography of the Subarctic Pacific Region, 1960-72. *Int. North Pac. Fish. Comm., Bull.* 33, 187 p.
- Huang, N. E. 1979. On the surface drift currents in the ocean. *J. Fluid Mech.* 91:191-208.

- Hubert, W. E., and T. Laevastu. 1965. Synoptic analysis and forecasting of surface currents. U.S. Navy Fleet Numerical Weather Facility, Monterey, CA. Technical Note 9, 47 p.
- Ingraham, W. James, Jr., and F. Favorite. 1968. The Alaskan Stream south of Adak Island. Deep-Sea Res. 15(4):493-496.
- Ingraham, W. James, Jr., and R. X. Miyahara. 1988. Ocean surface current simulations in the North Pacific Ocean and Bering Sea (OSCURS - Numerical Model). NOAA Tech. Memo. NMFS F/NWC-130, 155 p.
- Ingraham, W. J., Jr., N. Pola Swan, Y. Lee, R. Miyahara, and M. Hayes. 1983. Processing of FNWC daily sea level pressure data on NWAFC Burroughs 7811. REFM Program Doc. 19, 101 p. Northwest and Alaska Fish. Cent., Natl. Mar. Fish. Serv., NOAA, 2725 Montlake Blvd. E., Seattle, WA 98112.
- LaFond, Eugene C. 1951. Processing oceanographic data. U.S. Navy Hydrographic Office, Washington D.C. Pub. 614, 114 p.
- Larson, S. E. 1975. A 26-year time series of monthly mean winds over the oceans, Part 1, a statistical verification of computed surface winds over the North Pacific and North Atlantic. U.S. Navy Environmental Prediction Research Facility, Monterey, California. ENVPREDRSCWFAC Tech. Paper No. 8-75.

- McNally, Gerald J. 1981. Satellite-tracked drift buoy observations of the near-surface flow in the eastern mid-latitude North Pacific. J. Geophys. Res. 86(C9):8022-8030.
- Neumann, G. 1939. Triftstomungen an der Oberflache bei "Adlergrund Feuerschiff." Ann. Hydrogr. Mar. Meteor. 67:1-82.
- Reed, R. K. 1980. Direct Measurements of Recirculation in the Alaskan Stream. J. Phys. Ocean. 10(6):976-978.
- Reed, Ronald K., and J. D. Schumacher. 1987. Physical Oceanography. In: W. D. Hood and S. T. Zimmerman (editors), The Gulf of Alaska: Physical Environment and Biological Resources, p. 57-76. U.S. Gov. Print. Off., Washington, D.C.
- Samuels, W. B., N. E. Huang, and D. E. Amstutz. 1982. An oil spill trajectory analysis model with a variable wind deflection angle. Ocean Eng. 9:347-360.
- Weber, J. E. 1983. Steady wind- and wave-induced currents in the open ocean. J. Phys. Oceanogr. 13:524-530.
- Witting, R. 1909. Zur Kenntnie den vom Winde Erzeigtem Oberflachenstromes. Ann. Hydrogr. Marit. Met. 73, 193 p.